From the Division of Medical Imaging and Technology
Department of Clinical Science, Intervention and Technology

Karolinska Institutet, Stockholm, Sweden

INTRAVENOUS CONTRAST MEDIA OPTIMIZATION AT COMPUTED TOMOGRAPHY

Anders Svensson

Karolinska Institutet

Stockholm 2015

Published by Karolinska Institutet.

ISBN 978-91-7549-850-8

¨Energy and persistence conquer all things¨

Benjamin Franklin

ABSTRACT

The administration of intravenous contrast media (IV CM) is essential for detecting lesions at most computed tomography (CT) examinations. The overall aim of this thesis is to investigate different aspects of IV CM administration that may affect the quality of the CT examination.

In **Study I** a comparison was made between a low-osmolar contrast media (LOCM) iomeprol and the iso-osmolar contrast medium (IOCM) iodixanol, focusing on how they affect heart rate (HR), influence patient heat sensation and image quality during coronary computed angiography (CCTA). No significant difference in terms of HR interfering with the imaging protocol was observed. However, there was a larger number of arrhythmic heart beats (HB) observed when using LOCM in comparison to IOCM ($p < 0.001$). There was no statistically significant difference in image quality between the two CM. The experienced heat sensation was significantly stronger with LOCM in comparison to IOCM (visual analogue scale = 36 mm and 18 mm respectively, $p< 0.05$).

In **Study II** the variation in IV CM-enhancement in Hounsfield units (HU) in the liver and the aorta in relation to different expressions of body size was studied using two different CM (LOCM iomeprol and IOCM iodixanol). A significant relationship was observed for all studied body size parameters. Three parameters had a stronger correlation to the CM-enhancement; Body weight (BW, r= -0.51 and -0.64), body surface area (BSA, r= -0.54 and -0.65) and lean body mass (LBM, r= -0.54 and -0.59), but there was no statistically significant difference between those. Body height (BH), body mass index (BMI) and ideal body weight (IBW) had weaker correlations to CM-enhancement of the liver and the aorta. When adjusting for differences in weight, height, age and sex between the two groups there was a significantly stronger liver enhancement with iodixanol than with iomeprol (mean difference 6 HU, $p < 0.01$).

In **Study III** the correlation between liver CM-enhancement and volume pitch-corrected computed tomographic dose index ($CTDI_{vol}$) and BW was studied. Liver enhancement was negatively correlated to both $CTDI_{vol}$ ($r = -0.60$) and BW ($r = -0.64$).

In **Study IV** the relationship between arm positioning, BW and cardiac output (CO) versus CM-enhancement /timing during CCTA was studied. Patients were randomized into two groups. Group A (n=50) was positioned with arms resting on a pillow above their head and Group B (n=50) with their arms resting on the front panel of the CT. Statistically significant more patients in group A compared with group B (26 versus 14) showed a higher attenuation of the left atrium in comparison to the ascending aorta indicating too early scanning after IV CM injection ($p=<0.05$). In both groups BW and CO were statistically significantly related to the attenuation of ascending aorta ($p<0.01$).

Conclusion: The iso-osmolar contrast medium iodixanol causes less arrhythmic HB and less heat sensation than the low-osmolar contrast medium iomeprol, but this does not significantly influence the quality at CCTA. The positioning of the arms affects contrast media timing at CCTA. CM-enhancement of the liver and aorta is affected by body size. Several parameters can be used to adjust CM dose, but none is statistically significantly better parameter than BW. However, $CTDI_{vol}$ can potentially replace BW when adjusting CM dose for body size. This would make it potentially feasible to individualize CM dosage automatically by the CT scanner.

LIST OF PUBLICATIONS

I. **Heart rate variability and heat sensation at CT coronary angiography: Low-osmolar versus iso-osmolar contrast media.**
Svensson A, Ripsweden J, Rück A, Aspelin P, Cederlund K, Brismar B.T. *Acta Radiologica 2010;51(7):722-6*

II. **Hepatic contrast medium enhancement at computed tomography and its correlation with various body size measures.**
Svensson A, Jallo N, Cederlund K, Aspelin P, Nyman U, Björk J, Brismar B. T. *Acta Radiologica 2012; 53: 601–606*

III. **Automatic individualized contrast medium dosage at hepatic CT, by using computed tomography dose index volume ($CTDI_{vol}$).**
Svensson A, Cederlund K, Aspelin P, Nyman U, Björk J, Brismar B. T. *European Radiology 2014;24:1959-63*

IV. **Timing and enhancement of intravenous contrast media at coronary computed tomography angiography: The effect of arm positioning, body weight and cardiac output.**
Svensson A, Cederlund K, Aspelin P, Nyman U, Brismar B. T. *Submitted Journal of Cardiovascular Computed Tomography*

CONTENTS

1 Introduction 1
1.1 Background 1
1.2 Intravenous contrast media (CM) 2
1.2.1 The history of intravenous contrast media 2
1.2.2 Contrast media induced adverse reactions 2
1.2.3 The development of new intravenous contrast media 4
1.2.4 Optimization of contrast media enhancement at CT 4
1.3 Computed tomography (CT) 5
1.3.1 The development of spiral and multidetector CT (MDCT) technology 5
1.3.2 Dose concepts in CT 6
1.3.3 Automatic exposure control (AEC) 7
1.3.4 Image noise 8
1.4 Coronary computed tomography angiography (CCTA) 9
1.4.1 The development of ECG gated cardiac scanning 9
1.4.2 CCTA 64 row MDCT technique 10
1.4.3 Half scan technique 12
1.4.4 Dual source CCTA technique 13
1.4.5 Optimization of contrast media enhancement at coronary computed tomography angiography (CCTA) 13
1.4.6 Visual analogue scale (VAS) 14
1.4.7 Patient preparation and pitfalls in 64-row MDCT CCTA 15
1.5 Different body size measures 16
1.5.1 Body mass index (BMI) 16
1.5.2 Ideal body weight (IBW) 16
1.5.3 Lean body mass (LBM) 16
1.5.4 Body surface are (BSA) 16
1.6 CT liver imaging 17
1.6.1 Optimization of contrast media enhancement in liver 17
2 Aims of the thesis 19
3 Material and methods 20
3.1 Patients 20
3.2 Methods 22
3.2.1 Patient preparation (Study I, IV) 22
3.2.2 Patient preparation (Study II, III) 23
3.2.3 Scanning parameters and technique (Study I) 23
3.2.4 Scanning parameters and technique (Study II, III) 24
3.2.5 Scanning parameters and technique (Study IV) 25
3.2.6 Contrast medium administration (Study I) 25
3.2.7 Contrast medium administration (Study II, III) 26
3.2.8 Contrast medium administration (Study IV) 26
3.2.9 Visual analogue scale analysis (Study I) 26
3.2.10 Data analysis (Study I) 27
3.2.11 Image quality assessment (Study I) 27

3.2.12 Data analysis (Study II, III) 28
3.2.13 Data analysis (Study IV) 28
3.2.14 Statistics (Study I-IV) 28
4 Results and comments 30
4.1 Study I 30
4.1.1 Results 30
4.1.2 Comments 31
4.2 Study II 31
4.2.1 Results 31
4.2.2 Comments 34
4.3 Study III 34
4.3.1a Results, Group 1 34
4.3.1b Results, Group 2 35
4.3.2 Comments 36
4.4 Study IV 37
4.4.1 Results 37
4.4.2 Comments 38
5 Discussion 39
5.1 Heart rate variability and heat sensation at CT coronary angiography: Low-osmolar versus iso-osmolar contrast media (Study I) 39
5.2 Hepatic CM-enhancement at CT and its correlation with various body size measures (Study II) 40
5.3 Automatic individualized contrast medium dosage at hepatic CT, by using computed tomography dose index ($CTDI_{vol}$) (Study III) 41
5.4 Timing and enhancement of intravenous contrast media at coronary computed tomography angiography: The effect of arm positioning, body weight and cardiac output (Study IV) 41
6 Conclusions and final remarks 43
7 Acknowledgements 44
8 References 45

LIST OF ABBREVIATIONS

AA	Ascending aorta
AASLD	American Association for Study of Liver Diseases
AEC	Automatic exposure control
APASL	The Asian Pacific Association for the study of Liver
BH	Body height
BMI	Body mass index
BSA	Body surface area
BW	Body weight
CCTA	Coronary computed tomography angiography
CIN	Contrast media induced nephropathy
CM	Contrast medium
CO	Cardiac output
CT	Computed tomography
CTDI	Computed tomography dose index
$CTDI_{vol}$	Computed tomography dose index volume
$CTDI_{w}$	Computed tomography dose index weighted
DLP	Dose length product
ED	Effective dose
EBCT	Electron beam computerized tomography
ECG	Electrocardiogram
GFR	Glomerular filtration rate
HOCM	High osmolar contrast media
HB	Heart beat
HU	Hounsfield units
HR	Heart rate
IBW	Ideal body weight
IOCM	Iso-osmolar contrast media
IV	Intravenous
kVp	Peak kilovoltage
LBM	Lean body mass
LEVDP	Left end ventricular diastolic pressure
LMCA	Left main coronary artery
LOCM	Low osmolar contrast media
mAs	Milliampere second
MDCT	Multidetector computed tomography
mGy	Milligray
MHE	Maximum hepatic enhancement
P	Pitch
RCA	Right coronary artery
ROI	Region of interest
SSCT	Single slice computed tomography
SV	Stroke volume
Sv	Sievert
VAS	Visual analogue scale

1 INTRODUCTION

1.1 BACKGROUND

A computed tomograph (CT) produces images of the human body by mechanically rotating an x-ray tube and detector array around the patient. When passing through the body the photons in the x-ray beam are taken up differently depending on the density of the tissues. By continuously comparing the amount of photons leaving the x-ray tube with the number of photons detected by the detector when the x-ray tube rotates around the body the theoretical uptake of photons in different parts of the body can be calculated and an image can be constructed.

The inventor and constructor of this technology was the British-born electrical engineer Godfrey Newbold Hounsfield (28 August 1919-12 August 2004). Hounsfield grew up on a farm in Nottinghamshire, England. Based on descriptions from his early years on the farm emerges the image of a person with a thirst for knowledge and great experiment lust.

At the time of World War II in 1939, Hounsfield enrolled as a volunteer reservist in the Royal Air Force (RAF) and was during the first years to be included in a maintenance unit where he came to learn basic electronics and radar technology. During 1942 Hounsfield was further educated within the RAF and came to the end of the war in 1945 to serve as a radar instructor. Hounsfield left the RAF in 1946 for three years of study at Faraday House Electrical Engineering College in London, and in 1949 he was graduated as electrical engineer. Hounsfield who during the war worked with radar equipment from the Electric and Musical Industries (EMI) Ltd in Middlesex joined the company in 1949.

The first years at EMI, he worked on research and development of military radar technology. It was during these early years that Hounsfield became interested in computer technology, a work which continued throughout the sixties. After abandoning a less successful computer project Hounsfield was given the opportunity to figure out alternative commercial projects. One of these ideas, which he presented in 1967, was the pattern recognition which became the basis for the development of the first CT scanner. It was called the EMI-Scanner and it could at that time only be used for brain scans. The first clinical patient was examined 1st of October in 1971 at Atkinson Morley's Hospital, London, England.

For the development of the CT Godfrey N. Hounsfield and Allan M. Cormack (23 February 1924-7 May 1998) shared the Nobel prize in medicine and physiology in 1979. Hounsfield received the prize for the construction of the CT and McCormack for his work on the reconstruction algorithm. The attenuation unit describing the photon uptake is called Hounsfield units (HU) to honour the inventor. The HU is defined by the Hounsfield scale, in which air is -1000 HU (lowest possible) and 0 is defined by the attenuation of water. There is no upper limit of the scale (1-4).

1.2 INTRAVENOUS CONTRAST MEDIA

1.2.1 The history of intravenous contrast media

In January 1896, shortly after the discovery of x-rays by Conrad Wilhelm Röntgen, the first in vitro angiogram was performed by Haschek and Lindenthal using a solution of bismuth, lead and barium injected into the vessels of an amputated arm (5). During the beginning of 1900s attempts were carried out with different early contrast media (CM) for imaging the renal system.
In 1904 Wulff managed to image the urine bladder using retrograde infusion of bismuth subnitrate. The first successfully performed retrograde pyelography was made by Voelecker and Lichtenberg in 1905-06 using colloidal silver (Collargol). However, the high injection pressure could cause serious complications damaging the renal pelvis.
Attempts with other types of solutions, such as thorium nitrate, were carried out by Burns in 1915, but as with its forerunner severe complications occurred.
In 1923 Osborne and Rowtree showed that sodium iodide used for the treatment of syphilis could also be used as an intravenous (IV) CM for imaging of the urine bladder. The American physicist Moses Swick in cooperation between the two German chemists, Binz and Räth, deleloped the first commercial hydrophilic IV CM, Uro-Selectan (Schering-Kahlbaum) introduced in 1929 (6-7).

1.2.2 Contrast media induced adverse reactions

The only desirable effect wanted from IV CM is the attenuation of x-ray photons, all other effects is to be considered as secondary or toxic effects.
CM can be divided into four different groups; 1) ionic monomers 2) ionic monoacidic dimers 3) non-ionic monomers 4) non-ionic dimers (8) (Figure 1).

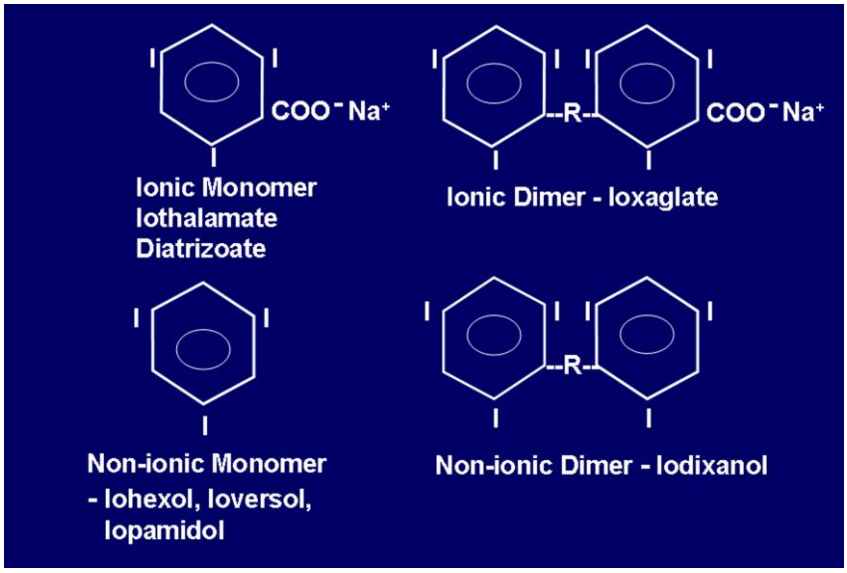

Figure 1. Chemical formulas of contrast agents (8).

CM toxicity refers to the sum of 4 influencing factors:

1) *Osmotoxicity*. Osmotic effects caused by a CM affect the water transport across cell membranes. The osmotic effect (Figure 2) of a CM is related to the ratio of iodine atoms per molecule. A higher ratio, ie more iodine atoms per molecule, causes a lower osmotic pressure and thereby a lower osmotoxicity. Previous angiographic studies have shown that high-osmolar contrast media (HOCM) cause more cardio and pulmonary events, such as increased heart rate and/or breathing rate, and vasodilatation resulting in a greater decrease in arterial pressure than low-osmolar contrast media (LOCM) do. The osmotoxicity of HOCM may also lead to crenation and decreased deformability of red blood cells resulting in microembolization with e.g. blockage of pulmonary circulation in patients with pulmonary hypertension. Osmotoxicity may also induce neurotoxic reactions such as spasm and unconsciousness. Moreover, the experienced heat sensation and pain in association with the CM injection has been shown to be substantially worse with HOCM (9-17).

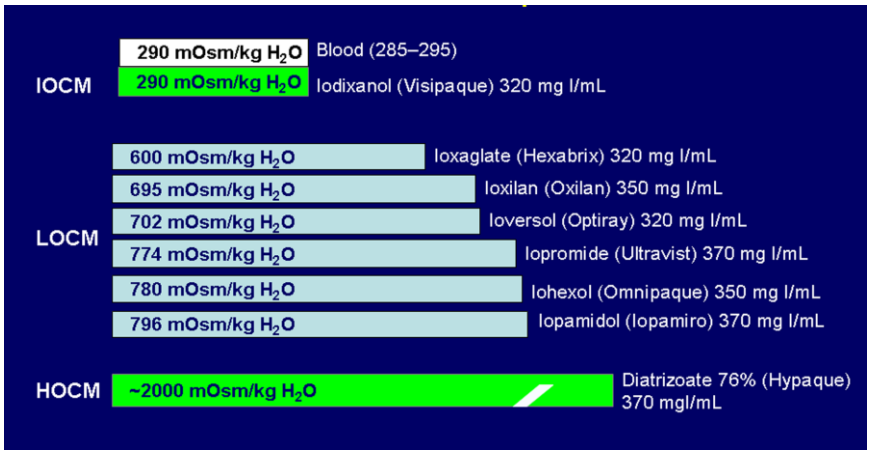

Figure 2. CM osmolalities, comparison chart (18-19).

2) *Ionic toxicity* refers to the electrolyte content of the CM. Changes in electrolyte concentrations may lead to a reduction in cardiac contractibility and/or induce arrhythmia, which in worse scenarios may lead to ventricular fibrillation. Different types of chelating agents of CM could affect the concentration of free calcium ions and thereby influence cardiac hemodynamic (8, 20).

3) *Viscosity* describes the ability of a fluid to resist flow. The viscosity of a CM is determined by its concentration and molecular size and shape. The chemical tolerance of the CM is also affected by the viscosity. Iso-osmolar (IOCM) have a greater viscosity in comparison to the same concentration of LOCM, i.e. high viscosity means thicker fluid, which may affect the possibility of using a high injection rate. Since viscosity also is dependent on temperature, heating of a CM can substantially decrease its viscosity and thereby facilitate higher flow rates (11, 21-24) (Table 1).

Table 1. CM dynamic viscosity (centipoise, cP) (24-25)
Higher cP value means increased CM viscosity

Contrast media	20°C cP	37°C cP
Iohexol (Omnipaque® 300mgI/ml)	11.8	6.3
Iodixanol (Visipaque®320mgI/ml)	26.6	11.8
Iomeprol (Iomeron® 400mgI/ml)	27.5	12.6

4) *Chemotoxicity* is the sum of osmo- and -ionic toxicity and viscosity which may affect normal cell functions by interaction with plasma proteins. This may cause hypersensitivity reactions by releasing vasoactive substances.
The chemotoxicity is affected by the number of hydroxyl groups which are added to improve the hydrophilic capacity of none-ionic CM (8-11).

The pH value of the IV CM is also of importance, where a low pH may lead to vasodilation and hypotension (8).

CM induced nephropathy (CIN) is considered as a complication to the use of CM. The complication predominantly affects patients with reduced renal function. The generally accepted threshold for increased CIN risk is defined as a glomerular filtration rate (GFR) <45ml/min/1.73 m² or the presence of multiple risk factors such as diabetes severe cardiac failure, chock and dehydration. Previous studies have shown a greater frequency of CIN when using HOCM in comparison to LOCM (26).

1.2.3 The development of new intravenous contrast media

Pioneer work during the 1960s performed by Torsten Almén lead to the development of the first non-ionic monomer LOCM metrizamide (Amipaque, Nygaard & Co, Norway) which was introduced in the 1970s.
In comparison to previously used ionic HOCM metrizamide demonstrated a significant reduction of all adverse reactions and almost eliminated pain associated with angiography. However, the sterilization process (autoclaving) made the CM molecule unstable when in solution so the CM had to be distributed as a powder to be mixed with water prior to the X-ray examination.
To avoid this inconvenience Nyegaard & Co marketed the LOCM non-ionic monomer iohexol (Omnipaque®) in the 1980s followed by the first IOCM, the none-ionic dimer iodixanol, (Visipaque®) during the 1990s. Iodixanol is isotonic to plasma, and cerebrospinal fluid at all concentrations (19).

1.2.4 Optimization of contrast media enhancement at CT

Although CT imaging was revolutionary for direct visualization of organs and pathology it could be further improved by using IV CM. The CM used in clinical practise are based on iodine. Iodine has a very high attenuation and CM can therefore be used to improve visualization of blood vessels, internal organs and

pathologic condition after their injection into the vascular system. The enhancement from the CM is defined as an increase in Hounsfield units (HU-enhancement).
The administration of CM during CT is today regarded as crucial for detecting parenchymal lesions. There are several physiological factors that affect the CM-enhancement where body size (defined by body weight, BW and body height, BH) and cardiac output (CO, defined on stroke volume (SV) and HR) are the most important. Other factors associated to the CM-enhancement is age, gender, hepatic cirrhosis, renal function, and portal hypertension. Also technical factors have great influence on CM-enhancement, e.g. x-ray tube potential, injection rate (ml/s) and CM volume (ml). To achieve the highest accuracy when detecting pathology at CT all these factors must be optimised (27-35).

1.3 COMPUTED TOMOGRAPHY (CT)

1.3.1 The development of spiral and multidetector CT (MDCT) technology

The development of spiral or helical CT technology during the end of 1980s and beginning of 1990s made huge impact on radiology. It was made possible by the introduction of the 'slip ring' technology in 1987 (Somatom Plus, Siemens Medical Systems, Germany and TCT 900S Thoshiba Medical Systems, Japan) that allowed the x-ray tube and detector to rotate without any power supplying cable interfering with the rotation. The spiral, or also so-called helical technique, was for the first time presented in 1989 and it replaced the old 'step and shoot' technique.

At spiral scanning there is a continuous x-ray tube and detector rotation during a continuous table movement. This lead to a significantly reduced scan time (36) and improved the examination quality by reducing motion artefacts. For the patients this also meant higher comfort, because breath hold duration could be reduced (37).
In order to describe the relationship between table movement per rotation and collimated slice thickness the concept of pitch (P) was introduced. At single slice CT (SSCT) P is calculated by dividing table movement (mm) per rotation with slice thickness (mm) (38).

In the end of 1990s the first multirow detector CT (MDCT) system was presented. The detector in these systems consists of several rows of detector elements. These reduce the scan time by increasing the coverage per rotation of the x-ray tube.
During the last decade CT vendors have presented MDCT systems with an increasing number of detector rows; from 4 to 16, 32, 64, 128, 256 to 320 rows (39--42).
At MDCT the calculation of P is different to that of SSCT. The P is calculated by dividing the table movement (mm) per rotation with the coverage, i.e. the total thickness of all simultaneously collected slices (nominal collimation) (38) (Table 2).
During the last few years dual energy MSCT systems have been introduced. With these systems the same anatomical section is scanned (almost) simultaneously with different x-ray tube potential (e.g. 80 and 140 peak kilovoltage (kVp) which potentially enables better tissue characterization. Example of applications for dual energy is urine stone characterization, gout diagnosis, bone subtraction, virtual non-contrast studies, dual energy cardiac perfusion, metal artefact reduction etc.

The technical solution behind simultaneously dual energy scanning is somewhat different between MDCT manufacturers. The Siemens Definition Flash system (Siemens Medical Systems, Erlangen, Germany) uses two separate x-ray tubes and detectors while the GE Discovery 750 HD (GE healthcare, Milwaukee, USA) uses fast kV-switching during the gantry rotation. The IQon Spectral CT from Philips (Philips healthcare, Best, Netherlands) uses a dual-layer detector where the top layer detects raw data with lower energies and the bottom layer higher energies (43-44).

Table 2. Pitch (P) formulas (38)

Pitch (P) formulas	
Single slice CT (SSCT)	$P = \frac{\text{Table movement per rotation (mm)}}{\text{Slice thickness (mm)}}$
Multi detector CT (MDCT)	$P = \frac{\text{Table movement per rotation (mm)}}{\text{n x T}}$ (n=slice thickness, T= total thickness of all simultaneously acquired slices)

1.3.2 Dose concepts in CT

Absorbed radiation represents the energy deposited per unit mass tissue, Joule per kilogram (J/kg). The absorbed radiation energy is measured in the unit Gray (Gy), where 1 Gy is equivalent to 1 J/kg.
The type of ionizing radiation used determines the biological effects per unit mass tissue. Due to this reason, different weighting factors for different radiation types are used. By multiplying the absorbed radiation energy, Gy, with the use of radiation type specific weighting factor, the dose equivalent expressed in the unit Sievert (Sv) can be calculated. The unit is named after Rolf Sievert who was a Swedish pioneer in science of radiation protection.

The CT Dose Index (CTDI) was established in the 1980s and it is used for standard measurement of radiation dose in CT. Using the $CTDI_{100}$ a 100 mm long pencil ion chamber is placed in multiple positions centrally and peripherally in a phantom, usually a 16-cm (head) or a 32-cm (body) phantom measuring the dose in Gy (at CT usually expressed in mGy). From these measurements the average dose is estimated and referred to as the weighted CT dose index ($CTDI_w$).
Because of large geometrical differences between the old ¨step and shot technique¨ and the spiral technique the concept of $CTDI_{vol}$ was introduced during the 90's. Unlike $CTDI_{w,}$ measuring mean radiation in a section (x, y direction), $CTDI_{vol}$ is pitch corrected and represents the mean radiation in a scanned volume (x, y and z direction).
The total absorbed dose for a scanned volume is calculated by multiplying $CTDI_{vol}$ with scan length in cm, referred to as the dose-length product (DLP). It is expressed in mGy cm (Table 3).

Table 3. CT dose formulas

	CT dose formulas
Pitch (P) corrected computed tomography dose index ($CTDI_{vol}$)	$CTDIvol = \frac{\text{CTDIw}}{\text{P}}$
Dose-length product (DLP)	$DLP = \text{CTDI}_{vol} \text{ x length (cm)}$

The body organs have different sensitivity to ionizing radiation. In order to estimate the risk from a single CT examination or to compare different types of x-ray examinations the effective dose (ED) is used. The unit for ED is Sv (common level used in radiology is mSv) (45-48).

1.3.3 Automatic exposure control (AEC)

Different vendor solutions for automatic exposure control (AEC) are present on the CT market (Table 4) (Figure 3). Common to all AEC systems is that they aim to adapt the radiation dose to the attenuation of the different parts of the individual patient. This means that both unnecessarily high doses of radiation and radiation starvation can be avoided, keeping the noise level constant throughout the scanned volume. AEC can be divided into three sub-groups;

Patient-size, AEC, is based on the overview image (topogram) where the tube current is defined by the patient's overall body size.

Z-axis AEC means that tube current is varied along the patient's z-axis. The technique is based on information from the overview image. The noise level is kept constant throughout the scanned volume by varying the tube current depending on the total amount of tissue (i.e. attenuation) along the z-axis.

Rotational or angular AEC means that depending on projection the tube current is varied during the rotation. The tube current is increased in the projections were the patient is widest (most often lateral view) and decreased in the projection where the patient is thinner (most often anterior-posterior, posterior-anterior view). Online modulation uses information from the previous 180° rotation and adjusts the current with a delay of 180° (49-50).

In order to have AEC to function as intended it is of utmost importance that the patient is centered in the CT gantry. Kaasalainen et al. reported 38% increased and 23% decreased radiation dose when the level of the examination table was at is highest versus lowest studied position (51).

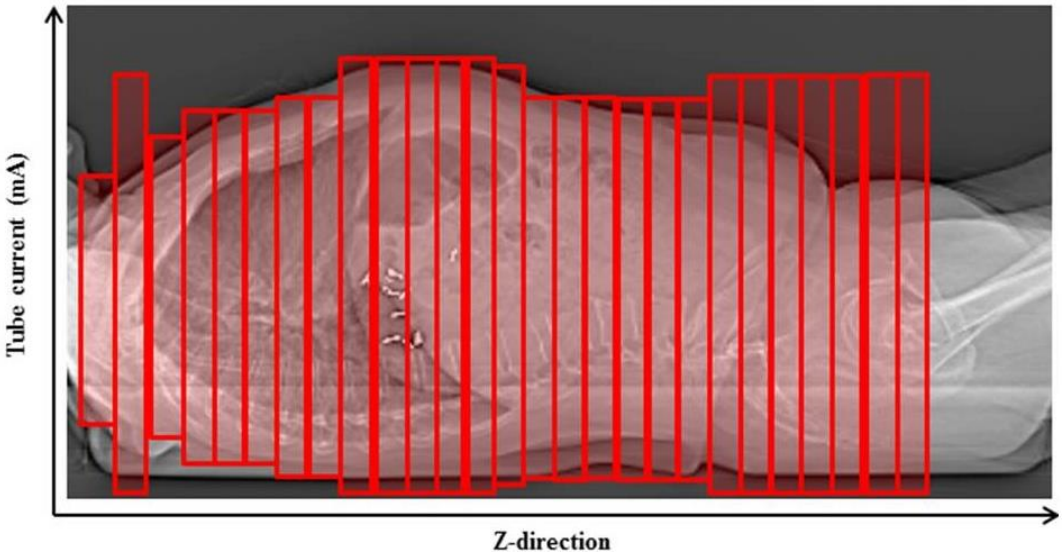

Figure 3. Automatic exposure control (AEC). Tube current is adjusted depending on the predicted amount of tissue in each projection along the scan.

Table 4. Automatic exposure control (AEC) of various CT manufacturers (50).

Manufacturer	Automatic exposure control (AEC) Patient size and Z axis-AEC* Angular AEC**
General Electric	AutomA* SmartmA**
Siemens	CARE dose 4D* **
Philips	DoseRight* **
Toshiba	Exposure 3D* **

Patient size and Z axis-AEC*, angular AEC**

1.3.4 Image noise

Image noise is defined as the standard deviation of the mean attenuation within a region of interest (ROI). Image noise plays a crucial role for the diagnostic sensitivity at CT to define pathology in of the parenchymal organs, especially in the detection of liver lesions.

Besides the tube current, image noise is affected by rotation time, tube potential (kVp), pitch, slice thickness, reconstruction kernel and electronic noise. The term signal-to-noise ratio (SNR) is defined as signal power divided by the noise level (SD). Thus, an increased radiation intensity to the detectors and thereby an increased dose to the patient reduces image noise while the inverse relationship applies to a reduction in radiation dose.

Another factor affecting the visualization of pathology is the image contrast between a lesion and the surrounding area. The so called contrast-to-noise ratio (CNR). It is defined as the difference between the mean HU measured in a lesion and its surroundings divided by the noise (SD) in the surrounding area. At least a minimum CNR level of 2-3 should be achieved to ensure proper diagnosis (Figure 4 a,b). To avoid the negative impact from image noise, x-ray tube potential (kVp) and loading (current x rotation in milliampere seconds (mAs) settings must be optimized (3, 52-53).

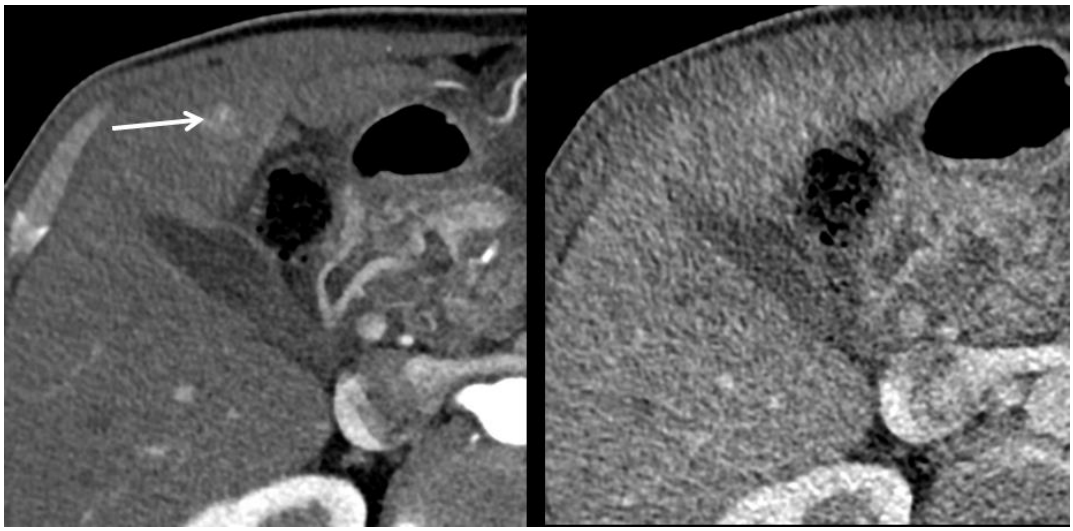

a **b**

Figure 4. (a) Hypervascular lesion (arrow), CNR 4.2. Same patient (b), CNR 1.2.

1.4 CORONARY COMPUTED TOMOGRAPHY ANGIOGRAPHY (CCTA)

1.4.1 The development of ECG gated cardiac scanning

In 1974 a research group in Japan under the leadership of Dr. Yo-ichhirou Umegaki, National Institute Radiation Science Tokyo, succeeded in performing the first ECG gated cardiac examination using electron beam computerized tomography (EBCT). Instead of using a conventional x-ray tube, the electrons were generated by an accelerator and then focused on targeted rings generating x-ray radiation. The technique was improved during the late 70s under the leadership of Dr. Douglas Boyd, UCLA, CA, USA, which led to the first commercial equipment to be introduced in 1980 (General Electric Imatron C 150). The temporal resolution, i.e. the acquisition time, was very fast in comparison with conventional CT scanners at that time. The main application for EBCT was to quantify calcifications in coronary arteries, so-called calcium scoring (Ca-scoring). However, the EBCT technique was expensive and it had a low spatial resolution, why the technique did not reach any general use.

The dynamic spatial reconstruction system (DSR) or the so called ¨The Mayo monster¨ was presented in the early 1980s. It was able to reconstruct 240 simultaneous 1mm slices collected from 14 separate x-ray tubes. The DSR system

was designed for visualization of heart and lungs, but because of its costs and size, 14 ton, DSR never became a commercial product.
The modern era of cardiac imaging started with the introduction of MDCT scanners in the late 1990s, when a shorter acquisition time and a better temporal resolution could be achieved. Since then the quality of cardiac imaging has continuously improved (54-56).

1.4.2 CCTA 64 row MDCT technique

In order to perform good cardiac imaging the contraction phase of the heart must be taken into account. This is achieved by using ECG gating / triggering. By recording the ECG signal the CT scanner can reconstruct images at the correct time intervals. There are two possible scanning techniques available;

Retrospective ECG-gating (spiral technique)

In the retrospective ECG-gating technique data is sampled during the whole R to R interval with the use of low pitch scanning (Figure 5). Due to this oversampling of data, images from all time points of the R to R interval can be reconstructed, which is important if changes in heart rate (HR) occurs during scanning. However, the disadvantage with this technique is the high radiation dose (57-58).

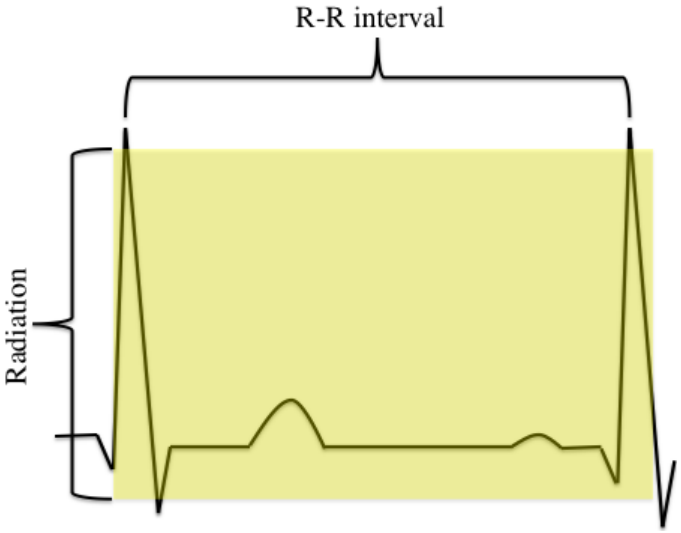

Figure 5. Retrospective ECG-gating. Spiral scanning through the whole R-R interval makes it possible to reconstruct data from every time point of the heart cycle.

To overcome this disadvantage, ECG dose modulation is used. The diastolic portion of the R to R interval is then scanned using a high radiation dose, allowing optimal image quality, and during the other parts of the cardiac cycle a lower radiation dose is used (59) (Figure 6). When the HR exceeds the scanning limits data are collected from more than one heart cycle. The disadvantage of this technique is that the image quality is very dependent on a stable heart rhythm (60).

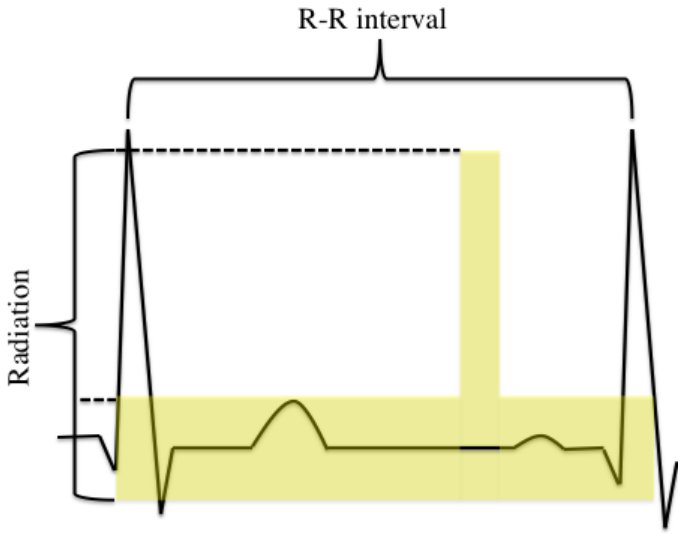

Figure 6. ECG-dose modulation. Highest mA-peak occurs at the diastolic part of the R to R interval.

Prospective ECG-gated technique (axial or ¨step and shoot¨ technique)

In the prospective ECG- gated technique a portion of the R to R interval is scanned (Figure 7). This results in about 80% lower radiation dose compared to that of the retrospective ECG-gated technique (61). However, motion artefacts may occur if the HR varies during the CCTA. That risk can be reduced by using the so-called padding technique (Figure 8). With this technique a data oversampling is used, i.e. a longer scanning period during the RR-interval than necessary compared to that of the ideal situation with a perfectly stable HR.
The temporal resolution varies between different types and / or generations of CT manufacturers. Previous studies have shown that the increased HR shortens the diastolic portion of R-R interval more than the systolic portion. This means that the scan window at prospective gating decreases with increasing HR while the systolic scan window is not affected to the same extent (62) (Figure 9 a, b).

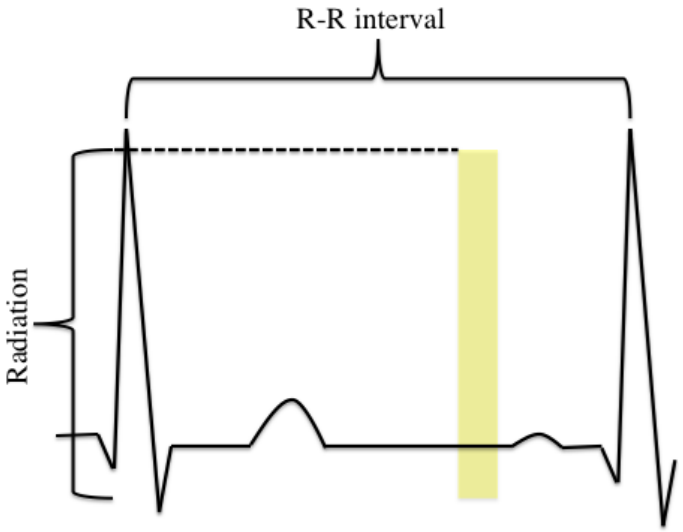

Figure 7. Prospective ECG-gating, axial or ¨step and shot¨ technique.
Scanning over a predefined portion of the R-R interval (diastole).

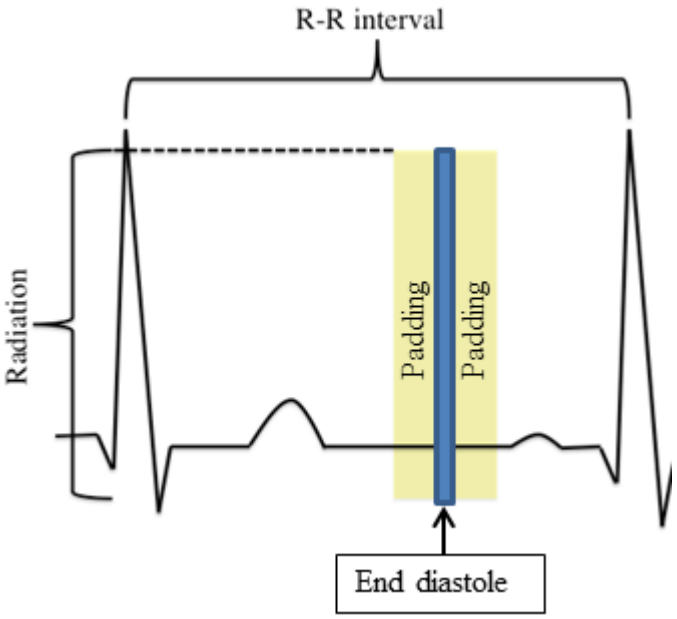

Figure 8. Prospective ECG-gating including padding technique. Padding refers to predefined scanning area (milliseconds or %) of every R-R interval.

a **b**

Figure 9. High quality CCTA examination showing left anterior descending artery (LAD) (arrow) (a) using prospective ECG-gating, systolic scanning (b) (arrows)

1.4.3 Half scan technique

To increase the temporal resolution at CCTA the so-called half-scan technique can be used. This means that data from only half a rotation is used to reconstruct the image. For example, when the time for a full rotation is 330 milliseconds (ms) the temporal resolution using the half scan technique will be 175ms (63-64).

1.4.4 Dual source CCTA technique

Unlike other suppliers of computer tomography equipment Siemens has developed a two detector array / x-ray tube system, e.g. the Somatom Definition Flash and Somatom Force. This represents a considerable improvement in performance in terms of CCTA temporal resolution (75ms and 66ms, respectively) in comparison with single array detector / x-ray tube systems.
The high performance of the dual source MDCT system enables CCTA examinations of patients with high and/or irregular HR. Studies where excellent image quality could be achieved in the patients with heart rates ranging between 70 and 110 beats per minute (bpm) using prospective technique have recently been published (65-67).

1.4.5 Optimization of contrast media enhancement at coronary computed tomography angiography (CCTA)

The aim of all IV CM injection protocols is to achieve sufficient attenuation of the coronary arteries. For clinical accuracy the attenuation of the coronary arteries should reach at least 300-400 HU (68). To obtain such a high contrast enhancement it is crucial to optimize the timing of the imaging in relation to the CM injection. There are two techniques to manage the timing of the imaging, the bolus tracking technique and the test bolus technique. At *bolus tracking* a monitoring image of the vessel of interest is obtained at predefined exposure interval. The CCTA then automatically starts when the attenuation in a region of interest (ROI), placed in the vessel by the operator, is higher than a predefined threshold.
At *the test bolus technique* a small amount of CM is injected and the time to maximal concentration (time to peak, TTP) is calculated from the monitoring images obtained during the test bolus. The TTP is then used to define the scan delay time for the CCTA examination (69-71).

Dual flow, or a so-called tri-phasic CM injection protocol, consists of three injection phases. The first phase is the pure CM bolus injection meant for enhancing the left side of the heart including the coronary vessels. The second phase is the mixed phase, saline and CM, with which the right side of the heart is enhanced. The third phase consists of a saline flush by which all CM is pushed forward, emptying superior vena cava from dense CM, preventing streak artefacts (Figure 10), (72-75).

For all used IV CM substances there is a potential risk of side effects. Studies performed during invasive coronary angiography (ICA) have shown a higher frequency of hemodynamic changes using HOCM in comparison to LOCM (76-79) (Figure 11). There have also been reports describing higher incidence of hemodynamic changes using LOCM in comparison with IOCM (80-81).
When the CM affects the hemodynamics it also affects the HR, and thereby the image quality. When the CM affects the hemodynamic changes it may also have an impact on patient discomfort. This has previously been observed in angiographic studies where a greater frequency of discomfort e.g. pain and heat sensation has been observed when using HOCM in comparison to LOCM (82). Similar results have been observed when using LOCM in comparison to IOCM (83-84).

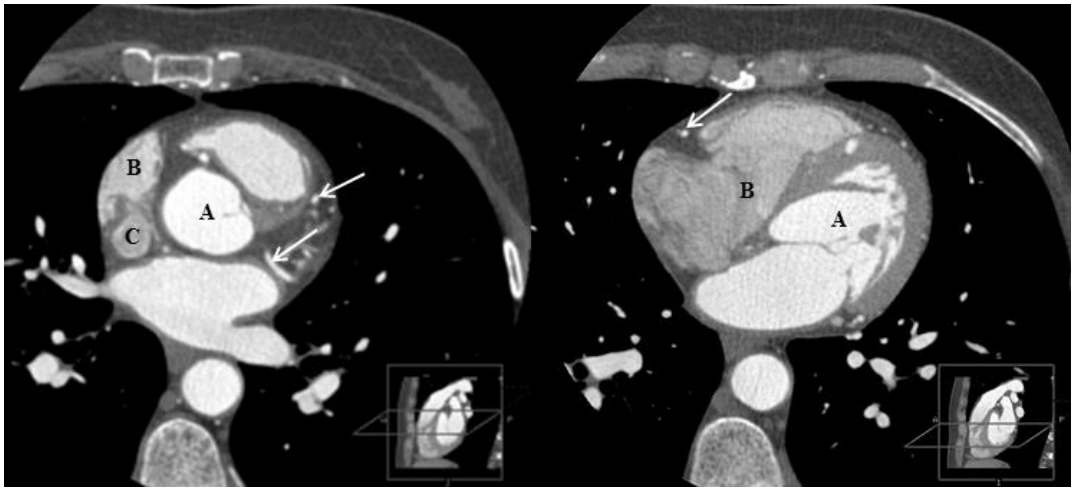

Figure 10. First CM injection phase (A) enhancing left side of the heart including coronary vessels (arrows). Second phase, mixed phase (B), enhancing right side of the heart. Third phase, saline flush emptying (C) superior vena cava from CM.

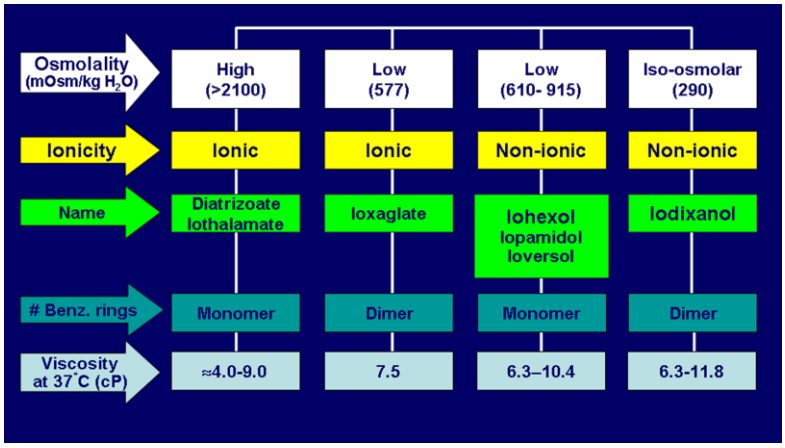

Figure 11. Intravenous contrast media classification (7, 85).

1.4.6 Visual analogue scale (VAS)

The use of the visual analogue scale (VAS) as a tool for measuring health outcome has been well established since the early 1970s. The phrase *feeling thermometer* was first expressed in the beginning of the 1980s and since then a number of different approaches for VAS have been created (length of line, scale marks, vertical or horizontal placement of the line, anchored endpoint of the line) (86-87).

In patient care the most common area for VAS is the estimation of pain. The original VAS-scale for evaluation of pain was constructed as a linear line (e.g. 100 mm) with endpoint headings; e.g. no pain versus the worst pain imaginable. The patient marks with a pencil a point on the line that corresponds to the experience of pain (88).

1.4.7 Patient preparation and pitfalls in CCTA

When performing CCTA a stable and low HR is of great importance to ensure optimal image quality (Figure 12 a,b). In order to reduce the heart rate ß-blockers are often used at CCTA imaging (89).

Patient specific parameters that affect image quality at CCTA are; HR and variability in HR, patient cooperation, patient size and calcified plaques. For an optimal CCTA study an ideal patient should therefore be non-overweight, able to follow the instructions, have a low and stable HR and have an absence of large coronary calcified plaques (90).

To obtain sufficient opacity of the coronary arteries a high CM bolus injection rate is required. Because the IV injection of CM is most often made through a peripheral vein catheter (PVC) a sufficiently coarse cannula is required, e.g. an 18-gauge PVC. In order to avoid high-density CM artefacts from the brachiocephalic vein, which may obscure the evaluation of the coronary arteries, the PVC should primarily be inserted on the right side (91). A better HU-enhancement is achieved when a proximal (antecubital vein) position is used compared to a distal position (34). Also, in case of CM extravasation the antecubital vein injection is safer in comparison to a distal injection site, e.g. hands.

It has been shown that the HR in average decreases about 4 heart beats (HB) during patient apnoea (92). The physiological reason for this is believed to be an increased parasympathetic stimulus of cardiac pacemaker cells (93). In order to select the most optimal scan protocol breathing exercises are made in association to the CT examination to determine the patient's breath hold capability and HR during apnoea.

As described above, the patient preparation and cooperation is of great importance for the outcome of CCTA. The presence of trained and experienced radiographers in this process has a great an impact on the correct selection of the scanning protocol, patient preparation and thereby the outcome of the scanning (91).

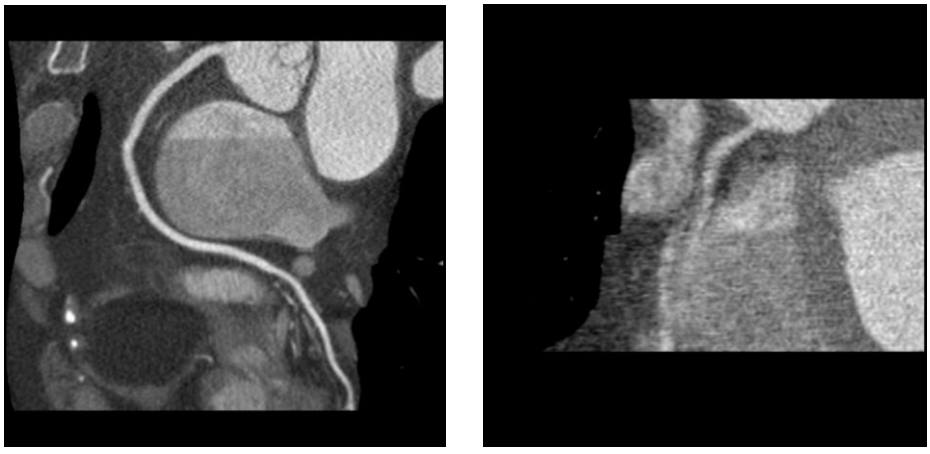

(a) **(b)**

Figure 12. Prospective ECG gated CCTA showing high image quality of the (a) right coronary artery (RCA). Hampered image quality of the RCA (b) due to motion artefacts and noise.

1.5 DIFFERENT BODY SIZE MEASURES

The classification of human body size has a long history, initially aiming on describing under- and overweight and also to define desirable or ideal body weight. During history obesity has been considered as a sign of good health. However, this opinion started to change during late 19th and early 20th century because of the observed complications associated to obesity. In 1913 one of the first height-weight tables were published based on data derived from actual measurements (with shoes and clothes on) of life insurance policyholders (94-95). Today, there are several models for measuring body size (Table 5).

1.5.1 Body Mass Index (BMI)

The probably most well-known model for measuring body size, besides body weight, is body mass index (BMI). The constructor of the equation was the Belgian mathematician and astronomer Adolphe Quetele (1796-1874). The equation became commonly used by American insurance companies during the period after the Second World War (96). Findings recorded by insurance statistical experts showed a clear relationship between obesity and increased mortality. Using that index, overweight is defined as a BMI of 25 to 30 kg/m^2 and obesity as a BMI above 30 kg/m^2 (97).

1.5.2 Ideal Body Weight (IBW)

The equation for ideal body weight (IBW) according to Devine was originally designed for the estimation of gentamicin clearance in obese patients. Due to the adverse effects associated with the accumulation of the antibiotic drug gentamicin, overdosing obese patients and/or patients with renal dysfunction could in worse cases lead to nephrotoxicity and ototoxicity (98). IBW has been shown to be superior to several other body measurements when calculating drug dosage in obese patients (99)

1.5.3 Lean body mass (LBM)

The parameter fat free mass, or more commonly lean body mass (LBM), refers to the total weight of muscles, organs and bones, excluding fatty tissue (100-101). The available technical methods for measuring LBM include whole-body densitometry by underwater weighing, bioelectrical impedance analysis (BIA), dual-energy x-ray absorptiometry (DEXA) and skinfold thickness (102). A simplified LBM can be calculated by using the formula developed by Hume (103) and by James (104). Those are both easily accessible but in comparison to technical measurement not as accurate (105).

1.5.4 Body surface area (BSA)

The equation for body surface area (BSA) was published by Du Bois & Dubois in 1916 (106). The equation is still commonly used in clinical practice, particularly for the calculation of chemotherapy doses and for normalizing parameters that varies with body size such as cardiac output, left ventricular mass and GFR (107-109). The equation was based measurements from a very limited number of subjects, only nine

adults, but it has been widely used over the years. A simplified equation for BSA was published in 1987 by Mosteller (110). The Mosteller formula has been shown to be more accurate than the previously used DuBois formula in the estimation of BSA in obese patients. The equation is also convenient to handle in daily clinical practice, being easily calculated using a pocket calculator (111).

Table 5. Body size equations

Equation	
Body mass index	Men and Women: Weight (kg)/(Height (m)^2)
Lean body weight, James (kg)	Men = 1.10 × Weight (kg) - 128 ×Weight^2/Height (cm)^2 Women = 1.07 × Weight (kg) - 148 × Weight^2/Height (cm)^2
Lean body weight, Hume (kg)	Men: 0.3281 × Weight (kg) + 0.33929 × Height (cm) – 29.5336 Women: 0.29569 × Weight (kg) + 0.41813 × Height (cm) – 43.2933
Ideal body weight Devine (kg)	Men: 50 + 2.3 × (Height (cm)/ 2.54 – 60) Women: 45.5 + 2.3 × (Height (cm)/2.54 – 60)
Body surface area Dubois (m^2)	Men and Women: 0.007184 × Height (cm)$^{0.725}$ × Weight (kg)$^{0.425}$
Body surface area Mosteller (m^2)	Men and Women: [Height (cm) × Weight (kg)/3600]$^{0.5}$

1.6 CT LIVER IMAGING

1.6.1 Optimization of contrast media enhancement in liver

Lesions in the liver are generally categorized as hypo or hyper vascular. In order to detect subtle differences in vascularisation between normal liver and pathologic lesions it is of great importance that the administration of the CM is optimal (112-115) (Figure 13 a,b).

Traditionally the same amount of CM has been given to all patients. However, the volume of distribution (VD) i.e. plasma and extravascular interstitial space into which the CM is diluted is related to the body size. Due to the low VD of adipose tissue the relationship between VD and body size is not linear. VD may therefore differ between two individuals of the same weight due to differences in body composition (116-118). A more individualized CM dosage has therefore been suggested. The goal is to achieve a more uniform CM-enhancement independent of body size (119). This would also reduce the amount of CM given to smaller patients, reducing the risk of side effects associated with CM can be reduced. This is especially important in elderly patients with reduced kidney function, i.e. a reduced glomerular filtration rate (GFR) (120).
Elderly patients often have a lower BW and therefore have a greater risk of CM overdose than younger patients. Several formulas have been proposed for calculating individual CM dosage based on body size (121-130), but there is no general agreement on which formula that results in the most optimal individual dosage.

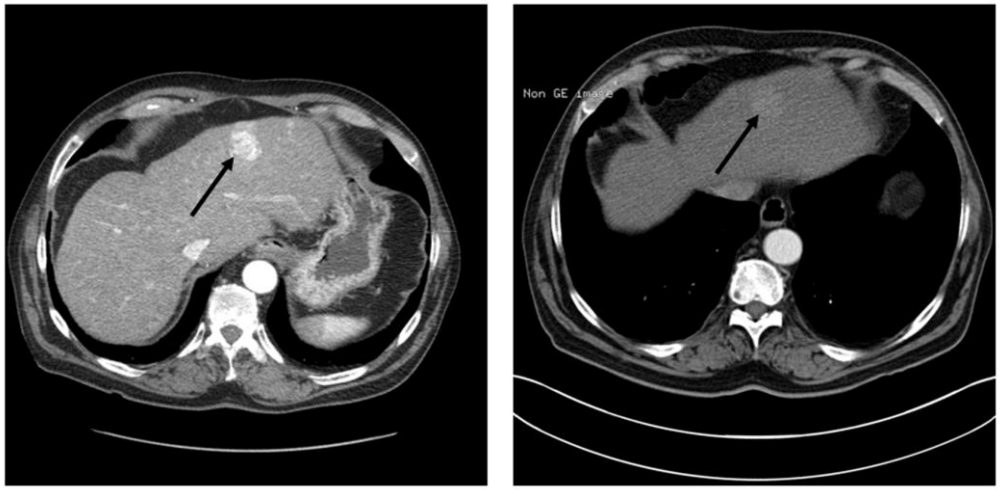

(a) **(b)**

Figure 13. Same patient scanned at two different hospitals. The arrow indicates a hypervascular liver lesion. Optimal CM timing and dosage (a), insufficient CM administration (b).

By using CM it is possible to rule out thrombosis of the liver vessels and to better depict tumours (131). By increasing the amount of injected iodine (gI) an improved CM-enhancement of the liver parenchyma can be achieved (132). For each patient the maximum hepatic enhancement (MHE) is desired, but the toxic side-effects must also be taken into account. In order to achieve a satisfactory diagnostic safety at least 50 HU enhancement is desirable (133-134).
Cardiac output (CO) (Table 6) is one of the physiological factors that may affect the CM-enhancement of the liver. Bae et al. showed that the time to MHE increased with 70s when CO was reduced with 55% (135). To compensate for the variation in CO so called bolus tracking is used in daily clinical practice (136) (see 1.4.5).
Improvements in the area of MDCT technology has made it possible to perform multiphase CM imaging, enabling the detection and characterisation of different focal liver lesions. For example, when diagnosing hepatocellular carcinoma (HCC) and intrahepatic cholangiocarcinoma there are consensus guidelines from the American association for study of liver diseases (AASLD) and the Asian pacific association for the study of liver (APASL) recommending a pre-contrast study, arterial phase, portal-venous phase and a delayed phase (¨wash out¨ phase) (137). However, the CM timing is crucial for the detection (138). When applying a two-phase liver CM protocol the typical delay in scanning, after reaching the threshold value in aorta, would be 15 seconds for detection of hypervascular lesions and 45 seconds for the detection of hypovascular lesions (139-140).

Table 6 . Cardiac function formulas (141)

Parameter	Equation
Cardiac output (CO)	CO = stroke volume (SV) x heart rate (HR) (mL/min) (mL/beat) (beats/min)

2 AIMS OF THE THESIS

The overall purpose of the research described in this thesis was to investigate how CM osmolality and body composition affects image quality and patient comfort.

Specific aims:

Study I: To evaluate whether an iso-osmolar contrast medium (IOCM, iodixanol) and a low-osmolar contrast medium (LOCM, iomeprol) affect heart rate (HR), HR variability, image quality and experienced heat sensation differently at coronary computed tomography angiography (CCTA).

.

Study II: To evaluate if any of the measures body height (BH), body mass index (BMI), lean body mass (LBM), ideal body weight (IBW) and body surface area (BSA) correlated better than body weight (BW) with hepatic contrast medium (CM) enhancement, and to compare the CM-enhancement when using iodixanol and iomeprol at multidetector row computed tomography (MDCT)

Study III: To evaluate hepatic parenchymal CM-enhancement during MDCT and its correlation with volume pitch-corrected computed tomographic dose index $CTDI_{vol}$) and BW.

Study IV: To evaluate the effect of arm positioning, BW and cardiac output (CO) on timing and CM-enhancement of intravenous (IV) CM at CCTA.

3 MATERIAL AND METHODS

3.1 PATIENTS

Study I: Between November 2005 and June 2007 100 patients scheduled for CCTA at Karolinska university hospital in Huddinge were enrolled in the study. In total 63 males and 37 females, aged 51-85 years with a mean age of 63 years were enrolled (Table 7).

Study II: Between November 2008 and February 2012 100 patients referred for IV CM thoraco-abdominal MDCT examination at Karolinska university hospital in Huddinge were enrolled in the study. Of the patients 58 were males and 42 were females, aged 35-89 years with a mean age of 64 years (Table 8).

Study III: In addition to the material in study II (group 1) another twenty patients (group 2) with 13 males and 7 females aged 54-80 years, mean age 69 years, were recruited to the study between January and February 2014 (Table 9).

Study IV: Between October 2013 and September 2014 100 patients referred for CCTA at the Karolinska university hospital in Huddinge were enrolled in the study. In total 66 males and 34 females aged 19-82 years with a mean age of 57 years were enrolled (Table 10).

In all studies patient body weight (kg) and body height (cm) were obtained and recorded, either by measurement with a wall-mounted ruler and a scale (Study II, III) or by questioning the patients and/or looking it up in the medical records (Study I, IV).

Exclusion criteria included earlier documented adverse allergic reactions to IV CM or an estimated GFR below 50 ml/min according to the Cockcroft-Gault formula based on the Lund-Malmö equation with lean body mass (142-143). In Study I atrial fibrillation and earlier by-pass surgery also constituted exclusion criteria.

All studies were conducted after approval from the local ethic committee at Karolinska Institutet and all patients gave their written consent.

All studies were evaluated on a dedicated workstation (Advantage work station 4.3, 4.5, GE Healthcare, Milwaukee, Wisconsin, USA).

Table 7. Patient characteristics (Study I) given as median values with 2.5 – 97.5 percentiles.

Parameters	All (n=100)	Women (n=37)	Men (n=63)
Age (years)	62 (51-78)	62 (51-76)	63 (52-78)
Body weight (kg)	78 (57-105)	69 (54-98)	82 (64-108)
Height (cm)	172 (157-188)	164 (154-172)	175 (161-188)
Body mass index (kg/m^2)	26 (21-35)	26 (21-36)	27 (21-34)
Lean body mass (kg)	54 (46-65)	53 (45-64)	55 (46-65)
Ideal body weight (kg)	63 (52-77)	61 (51-68)	66 (53-78)
Body surface area Mosteller (m^2)	1.93 (1.61-2.31)	1.76 (1.55-2.09)	2.0 (1.71-2.32)

Table 8. Patient characteristics (Study II) given as median values with 2.5 – 97.5 percentiles.

Parameters	All (n=100)	Women (n=42)	Men (n=58)
Age (years)	65 (35-84)	65 (36-78)	66 (35-86)
Body weight (kg)	72 (50-112)	65 (50-107)	80 (53-112)
Height (cm)	170 (155-190)	166 (153-175)	176 (162-192)
Body mass index (kg/m^2)	24 (18-35)	24 (18-36)	25 (18-34)
Lean body mass (kg)	53 (41-77)	46 (40-55)	61 (45-79)
Ideal body weight (kg)	65 (48-84)	57 (46-66)	71 (58-86)
Body surface area Mosteller (m^2)	1.83 (1.52-2.38)	1.72 (1.52-2.26)	1.96 (1.56-2.45)

Table 9. Patient characteristics (Study III) given as median values with 2.5 – 97.5 percentiles.

	Group 1 Same contrast media dose			Group 2 Individualized contrast media dose		
Parameters	All (n=100)	Women (n=43)	Men (n=58)	All (n=20)	Women (n=7)	Men (n=13)
Age	65 (35-84)	65 (36-78)	66 (35-86)	69 (55-80)	67 (60-80)	72 (55-79)
Weight	72 (50-112)	65 (50-107)	65 (50-107)	76 (52-116)	62 (52-73)	85 (56-118)
$CTDI_{vol}$	7.2 (4.2-28.3)	6.6 (4.2-23.9)	11.7 (4.5-22.9	10.7 (4.9-25.6)	8.4 (5.2-10.7)	14.3 (5.2-26.5)

Table 10. Patient characteristics (Study IV) given as median values with 2.5 – 97.5 percentiles.

Parameters	Group A (n=50)	Group B (n=50)	Probability
Age (years)	58 (12)	57 (13)	NS
Female/Male	17/33	17/33	NS
Body weight (kg)	76.1 (12.0)	75.9 (12.4)	NS
Body height (cm)	176.7 (10.2)	175.2 (10.2)	NS
Cardiac output (CO,mL/min)	4.2 (0.8)	4.4 (1.1)	NS
Heart rate (BPM) n=49	58 (9)	62 (9)	P<0.05

3.2 METHOD

In Study I, II, III all examinations were performed using a 64 row detector GE Light Speed VCT (GE Healthcare, Milwaukee, Wisc., USA).

In Study IV the examinations were performed using a dual source 2x64 row MDCT Siemens Somatom Definition Flash (Siemens healthcare, Forchheim, Germany).

In all studies a dual head auto injector (Medrad, Stellant Dual Head Injector, Pittsburgh, Pa., USA) was used for all IV CM injections. Two IV CM were used in Studies I, II and III; one IOCM (iodixanol 320 mg I/ml, Visipaque®, GE Healthcare, Chalfont St Giles, UK) and one LOCM (iomeprol 400 mgI/ml, Iomeron ® , Bracco Imaging SpA, Milan, Italy). In Study IV the IOCM iodixanol 320 mg I/ml was used IV CM.

3.2.1 Patient preparation (Study I, IV)

Patients were informed in writing to avoid nicotine and caffeine for 4 hours prior to the CT examination in order to avoid the effect on HR that these substances otherwise may had caused (144-145). At the CT suite one 18-gauge peripheral venous catheter was inserted in the right or left antecubital vein and connected to the syringes via a tubing catheter to the CM injector.

ECG leads were placed in Study I at the middle of both clavicle bones and in the left thoracic position and in Study II as above and also in the right thoracic position.
Breathing exercise maneuver took place with the patient positioned on the CT examination table. The breathing instructions for Study I was: Breath in deeply and hold your breath. Instructions for Study IV was: Breath in/out, breath in and then stop breathing
The breathing exercise was executed for controlling the breath hold capacity and for observing and recording the HR during apnea.

Study IV: Using sealed envelopes the patients were randomized into two groups with 50 patients in each.
Group A (n=50): Arms were positioned, above (superior) the head resting on a pillow during CM injection (Figure 14a). To avoid clamping of the peripheral cannula, patients were asked to hold their arms as straight as possible
.
Group B (n=50): Hands were resting on the CT front panel approximately 90 degrees ventral to the body (Figure 14b).

Figure 14a 14b

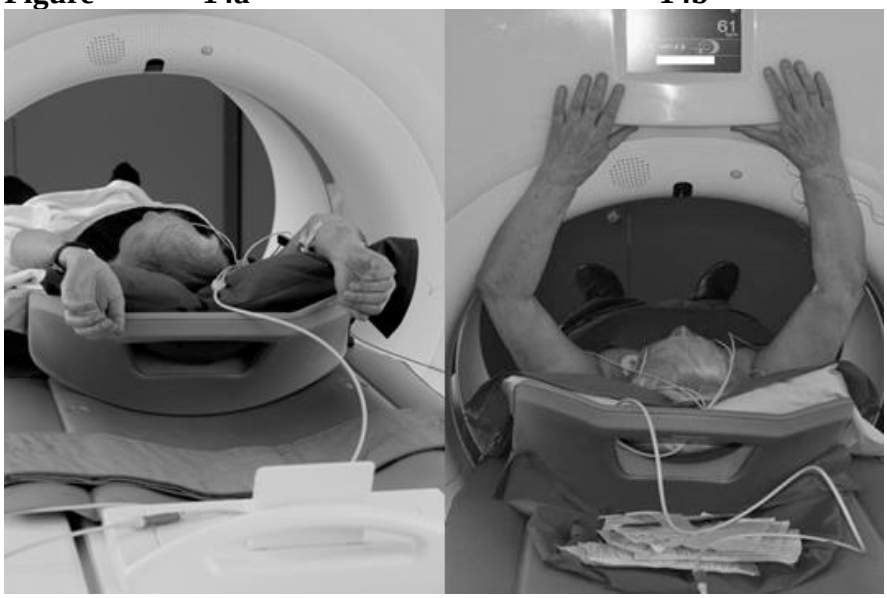

In group A the arms were positioned, above (superior) the head resting on a pillow during CM injection (Figure 14a) and in group B the hands were resting on the CT front panel approximately 90 degrees ventral to the body (Figure 14b).

Unless medically contraindicated, oral metoprolol (Seloken®, AstraZenica) was given one hour prior to the CCTA examination. In patients with HR of 60-65 beats per minute (BPM) 50 mg was given and 100 mg was given when > 65 BPM. Sublingual glyceryl trinitrate 0.4 mg/dose (Glytrin®, Meda AB)was given approximately 4-5 minutes before CCTA scanning to patients without contraindications.

3.2.2 Patient preparation (Study II, III)

BW was obtained in light clothing (underwear) using a medical balance (Soehnle professional, GMBH Company, Germany) and BH was obtained in the standing position without shoes using a dedicated wall-mounted ruler. An 18 gauge peripheral venous access was inserted into the right or left antecubital vein.

3.2.3 Scanning parameters and technique (Study I)

All CT examinations were performed using the retrospective segmental ECG gated scanning technique, which means that every single reconstructed image originates from one single heart cycle. The tube potential was set to 120 kVp for all examinations and ECG modulated tube current was used with the highest current peak (650 mA) at 70-80% of the R-R interval and the lowest was set to 250 mA when outside the predefined diastolic interval (Figure 15).

For each patient the scanning protocol was chosen based on the recorded HR during the apnea exercise prior to scanning. There were five different protocols, based on five different ranges in HR, each with a pitch optimized for that HR (Table 10). The scan range was planned on anterior-posterior and lateral overviews with the start

position at the level of the tracheal bifurcation covering the whole heart during patient apnea. The patients were asked approximately 10 seconds before scan start to take a deep breath and then to stop breathing.

All sampled data were retrospectively reconstructed into datasets visualizing the heart in 10% phases (0-90%) during the entire heart cycle. The obtained images in the data sets had a 0.625 mm slice collimation and a 0.625 mm increment.

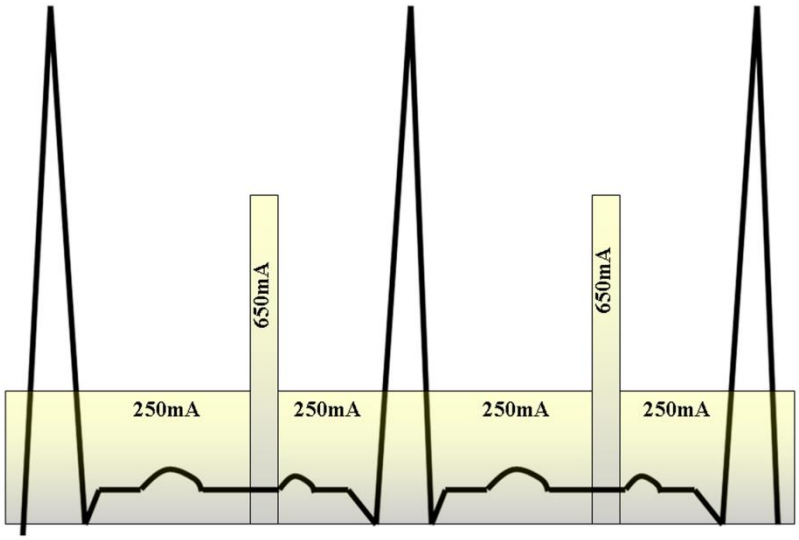

Figure 15. ECG dose modulated retrospective gating with the highest mA peak applied at 70-80 % of the R-R interval.

Table 11. The selection of pitch to use was based on heart rate recorded before scanning.

Heart rate	Pitch	Iodixanol (no. of patients)	Iomeprol (no. of patients)
30-40	0.16	2	0
41-49	0.18	6	9
50-57	0.20	12	12
58-65	0.22	16	11
66-74	0.24	14	18

3.2.4 Scanning parameters and technique (Study II, III)

All examinations were executed during apnea using a 120 kVp and automatic dose modulation (Smart mA, Auto mA), ranging from 100 mA to 700 mA, rotation time 0.5 s.
The scanning procedure included a three-phase protocol at a 64 x 0.625 mm detector collimation. The native phase was obtained with a noise index (NI) of 50 and a pitch of 1.375. The CM phases, late arterial phase (portal venous inflow phase) and the liver parenchymal phase, were conducted with NI 36 and pitch 0.984. Scan start for

the CM phase was defined by using bolus tracking technique (smart prep), where the triggering ROI was placed in the thoracic aorta at the level of the aortic arch. For the late arterial phase scan start was set to 20 seconds post threshold value of 150 HU, another 25 seconds were added for the liver parenchymal phase. All sampled data were reformatted to 5 mm thick slices with a 2.5 mm reconstruction overlap.

3.2.5 Scanning parameters and technique (Study IV)

Scanning parameters were as follows: 100 kVp, automatic dose modulation, quality reference 370 mAs, 64 x 0.6 mm detector collimation and 0.28 seconds rotation time, prospective ECG gating (segmental scanning).
CO and HR measurements were obtained before scan start, during test bolus injection, CCTA examination and after scanning using dedicated CO equipment (ICON^{TM}, Osypka Medical GmbH, Berlin, Germany).

3.2.6 Contrast medium administration (Study I)

Using sealed envelopes the patients were randomized prior to the CCTA examination to either receive pre-heated CM either iodxianol 320 mg I/ml or iomeprol 400 mg I/ml. The optimal scanning window was defined by using a test bolus injection protocol containing 20 ml of CM and 20 ml of physiological saline (NaCl) with the injection rate of 5 ml/s. Time to peak enhancement of ascending aorta was calculated by using a 20 mm circular region of interest (ROI). In order to compensate for the larger amount of CM used in the CCTA examination, compared to the bolus, a 7second delay was added to the calculated time to peak. During the CCTA examination the same CM volume was injected at 5 ml/s for both iodixanol and iomeprol by applying a 3-phase injection protocol. During the first phase a 50 ml CM bolus was used, then during the second phase a mixture of 20 ml CM and 30 ml of physiological NaCl was injected, followed by a 50 ml physiological NaCl flush during the third phase.

3.2.7 Contrast medium administration (Study II, III)

The studies were carried out with the injection of two different CM. A CM dose of 40 grams of iodine with a duration time of 25 second were used, e.g. 125 ml of iodixanol 320 mgI/ml with injection rate of 5 ml/s or 100 ml of iomeprol 400 mgI/ml at a rate of 4 ml/s. This resulted in an injected dose rate of 1.6 gram-iodine per second for both CM. The CM injection was followed by a 50 ml saline flush with injection rate corresponding to the CM injection.

Group 2 (n=20) (Study III): For this group of patients an individualized IV CM dosage (iomeprol 400 mg I/ml) was calculated on basis of the latest overview image projected $CTDI_{vol}$ value. The CM dose was adjusted so that 95 % of the patients would obtain a hepatic enhancement of at least 50 HU during the hepatic phase.

The equation for individually adjusting CM dose in **Group 2** using $CTDI_{vol}$ was based on the observations made in group 1 and calculated to:

$$\text{CM dose for woman (in grams)} = \frac{2600}{-1.16 x CTDI_{vol} + 74.3}$$

$$\text{CM dose for men (in grams)} = \frac{2600}{-1.38 x CTDI_{vol} + 81.3}$$

3.2.8 Contrast medium administration (Study IV)

The CCTA CM delay time was defined by using the test bolus technique with a bolus of 15 ml iodixanol 320mgI/ml.
Monitoring scans were obtained every 1 second. A delay of 2 seconds was added to the TTP automatically calculated by the CT scanner analysis program (Figure 16) from a 10 mm ROI placed in the ascending aorta.
At the CCTA examination, 60 ml of CM (iodixanol 320mgI/ml) followed by a 50 ml saline injection with a constant injection rate of 6 ml/s was used.

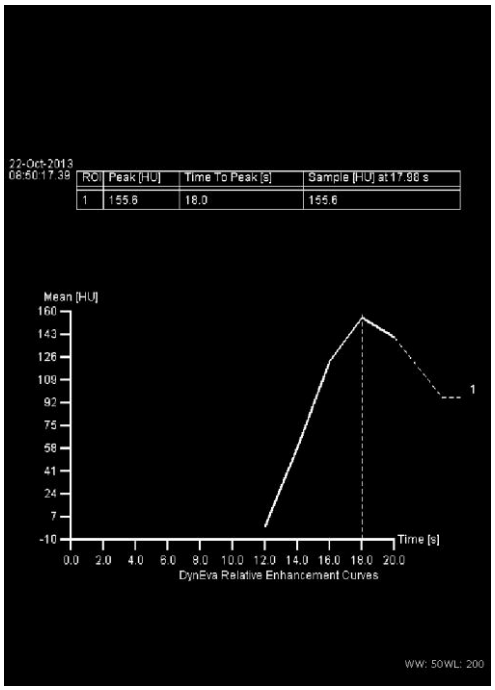

Figure 16. Time to peak (TTP) were automatically calculated by the CT scanner analysis program.

3.2.9 Visual analogue scale analysis (Study I)

After completing the scanning procedure the patients were asked to fill in a questionnaire using the visual analogue scale (VAS) regarding their experience of heat sensation associated with the CM injection. The scale ranged from "none" to "worst possible", where no experience of heat was 0 mm and the worst possible heat sensation was 100 mm (83) (Figure 17). The sensation experienced was marked using a pencil. The scale was then measured using a dedicated ruler.

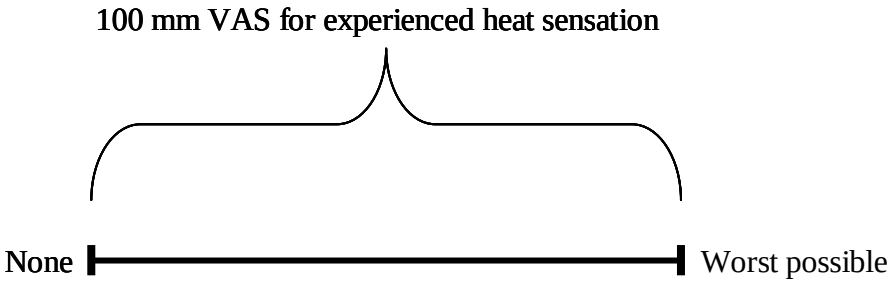

Figure 17. Visual analogue scale (VAS) for experienced heat sensation.

3.2.10 Data analysis (Study I)

During scanning the HR was automatically recorded using CT ECG leads. The CT system stored the heart rate obtained for each HB with the respective image and it was automatically written out on the displayed images at evaluation.

To obtain the individual HR and its variation during scanning, the following method was used. The table position and displayed HR at the position 20 mm superior to the origin of the LAD were noted. The images were then reviewed and the positions when the HR changed were recorded until to the most inferior image of the heart. Each position where a change in HR occurred indicated a new HB.

The total number of HB faster than 80 and faster than100 HB/min was counted for each CM. The deviation in individual HR from the permitted HR range defined in the scan protocol (Table 10) was noted for each HB, and the mean absolute deviation was calculated for each CM.

3.2.11 Image quality assessment (Study I)

The structure for the assessment of the coronary vessels was the same as that used for invasive coronary angiography (ICA). The coronary vessels were thereby divided into 18 segments (146). By the use of a three-point scale (excellent, acceptable and not diagnostic) the evaluation of the segments was conducted by two radiologists with 10 and 20 years of experience in radiology. The readers were blinded to all scan and clinical parameters. For the assessment of image quality they both used individualized window settings where window width (WW) ranged between 800-1200 HU and window level (WL) between 100-200 HU.

3.2.12 Data analysis (Study II, III)

A circular ROI with a diameter of about 10 mm was used. The attenuation in aorta was obtained at the level of the liver hilum before CM administration (native phase) and during the late arterial phase. The attenuation of the liver was obtained in the native and the hepatic parenchymal phase from ROIs placed in:

1) -central part of the liver

2) - liver 3 cm caudal to the hemidiaphragm

3) -liver 3 cm cranial to the caudal edge of the liver.

Care was taken to avoid partial volume effects and not to include any visible vessels nor areas with inhomogeneous attenuation in the liver. The CM-enhancement was calculated as the attenuation after contrast media subtracted with the attenuation in native phase.
The mean value of the three measurements was used for correlations made in Study II for BW, BH, BMI, LBM, IBW, BSA and in Study III BW and $CTDI_{vol}$.

3.2.13 Data analysis (Study IV)

The attenuation of the ascending aorta at the level of the origin of left main coronary (LM) artery, left atrium and inferior vena cava was obtained by placement of a 10-mm diameter ROI.
The ROI measurement of the inferior vena cava was performed to detect any hemodynamic differences that could affect the outcome between groups A and B. The recorded data from the CO equipment were transferred to an Excel spreadsheet for calculation and analysis of HR, stroke volume (SV) and CO.

3.2.14 Statistics (Study I-IV)

Differences in obtained parameters between groups were tested using Student's *t* test and differences in number of tachycard HB or number of patients with arrhythmia (Study I), or too early imaging (Study IV) was tested by using Fisher's exact test.

Difference in image quality and for median and mean differences in aortic and hepatic enhancement of the two different CM was tested using the Mann – Whitney U test (Study I and II). Relationships were calculated using linear regression analysis. Linear regression was also employed to adjust the differences in the enhancement of males and females and of the two different CM for differences in age, weight and height.

For the analysis of liver enhancement in Study III, linear regression analysis was used as dependent variable with either $CTDI_{vol}$ or BW as the main independent variable.
Correlations were described using Pearson's correlation coefficient r. Adjusted r^2 was used as a measure of the proportion of explained variance in the regression models. Differences for the overall data set in the correlations for BW versus any measures of body size with a higher correlation coefficient than BW was tested by

comparing squared unstandardized regression residuals from univariate linear regression analyses using the Wilcoxon signed-rank test (Study II).
The Fisher r- to –z transformation was used to test differences in correlation between males and females (Study II).

The effect of simultaneously including BW and $CTDI_{vol}$ were also included in the evaluation of data in Study III. Gender (male/female), BH and age on continuous scale were added as covariates. Wald test was used for the calculation of statistical significance.

For all studies p-values <0.05 were considered significant.

4 RESULTS AND COMMENTS

4.1 Study I

4.1.1 Results

There were no significant differences between the LOCM group and the IOCM group in HR, number of patients with a HR interfering with the scanning protocol, HR variability nor variability in HR interfering with the scanning protocol (Table 12). However, there was a significantly higher incidence of arrhythmic HB exceeding the thresholds 80 and 100 HB when using LOCM in comparison to IOCM). Patients receiving LOCM scored a higher heat sensation than those receiving IOCM (Figure 18).

There were no significant differences between the LOCM group and the IOCM group in number of diagnostic segments (514 vs 492) nor segments affected by movement artefacts (153 vs. 167). Analysis of the proportion of segments affected by movement artefacts and the deviation from pre-defined scanning protocol showed a significant relationship ($r=0.29$, $p<0.01$).

Table 12. Average heart rate during CCTA.

Parameter during CCTA	LOCM	IOCM
Increased HR (n)	21	16
Decreased HR (n)	14	12
Both increased and decreased HR (n)	4	0
Mean variance in HR (HB/min)	4.4 (SD 10.9)	1.4 (SD 3.4)
Total deviation in HR from the scan protocol (HB/min)	4.7 (SD 12.0)	2.0 (SD 4.1)
Number of arrhythmic HB exceeding the thresholds:		
80 HB	26	3
100 HB	15	1

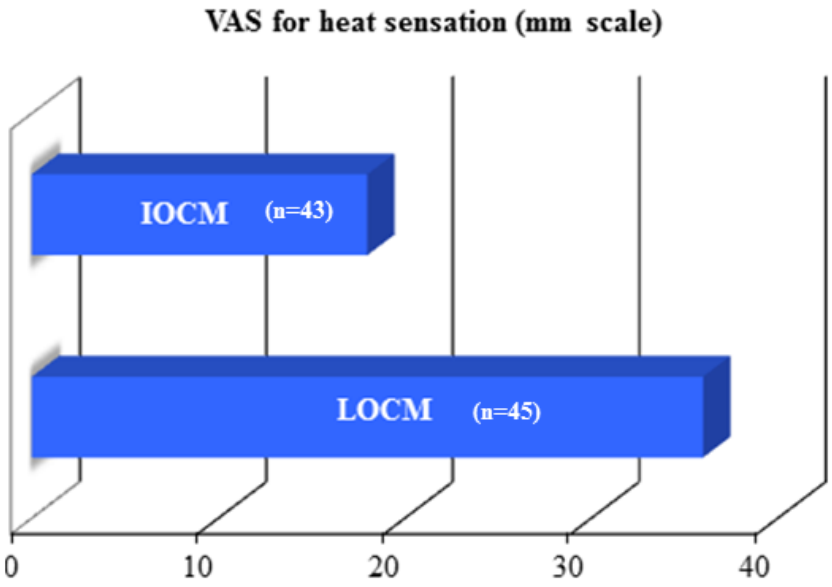

Figure 18. The difference in VAS between IOCM and LOCM in relationship to experienced heat sensation.

4.1.2 Comments

In our study the injected volume of CM was the same for LOCM and IOCM. However the total amount of iodine was larger with the use of LOCM iomeprol (400 mgI/ml) in comparison to iodixanol (320 mgI/ml) which resulted in a median or mean difference of 5.6 gram between the two CM. This may be considered as a limitation but the alternative was to use different injection rates, which at that time point was cumbersome. The two radiologists, who were blinded to which CM was used, could neither observe any significant difference in terms of image quality.

Of the 100 examined patients in Study I, 83 were on prescription of β-blockers (41 in the LOCM group and 42 in the IOCM group). In connection with the CCTA examination 5 of the otherwise untreated patients received intravenous β-blocker (3 in the LOCM group and 2 in the IOCM group).

4.2 Study II

4.2.1 Results

There was a wide inter patient variation in aortic and hepatic CM-enhancement; between 93 and 404 HU in the aorta and between 37 and 91 HU in the liver (95% percentile range) (Table 13). All studied body size parameters were statistically significantly negatively related to aortic and hepatic CM-enhancement (Table 14, 15), but three parameters showed a stronger influence on CM-enhancement, BW Figure 19, BSA (Figure 20) and LBM.
Gender did not have any significant influence on the relationship between body size measures and CM-enhancement.

Iodixanol and iomeprol, had a similar mean CM-enhancement in the aorta and the liver (Table 16), but when adjusted for weight, height, age and sex, iodixanol caused significantly stronger liver enhancement than iomeprol (mean difference 6 HU, $p < 0.01$).

Table 13. Attenuation and contrast medium enhancement of the aorta and liver expressed in Hounsfield Units (HU). Median values with 2.5 – 97.5 percentiles.

Parameters	All (n = 100)	Females (n=42)	Males (n = 58)
Aorta			
-native phase (HU)	37 (23-49)	39 (29-48)	35 (20-48)
-late arterial phase (HU)	252 (125-452)	305 (168-466)	231 (120-425)
-enhancement (HU)	217 (93-404)	265 (129-424)	188 (88-384)
Liver			
-native phase (HU)	57 (33-70)	60 (31-71)	56 (37-63)
-parenchymal phase (HU)	119 (83-152)	129 (83-153)	115 (84-143)
-enhancement (HU)	63 (37-91)	68 (44-92)	59 (36-87)
-enhancement <50 HU	n = 11	n = 2	n = 9

Table 14. Pearson's correlation coefficient regarding aortic enhancement in late arterial phase in relation to various body size measures.

Parameters	All (n=100)	Women (n=42)	Men (n=58)
Body weight (kg)	-0.51	-0.38	-0.50
Height (cm)	-0.44	-0.15	-0.43
Body mass index (kg/m^2)	-0.35	-0.32	-0.37
Lean body weight, James (kg)	-0.54	-0.42	-0.54
Ideal body weight (kg)	-0.45	-0.15	-0.43
Body surface area Mosteller (m^2)	-0.54	-0.40	-0.53

All correlation coefficients were statistically significant at the $p<0.0001$ level.

Table 15. Pearson's correlation coefficient regarding hepatic enhancement in the parenchymal phase in relation to various body size measures.

Parameters	All (n=100)	Women (n=42)	Men (n=58)
Body weight (kg)	-0.64	-0.66	-0.57
Height (cm)	-0.45	-0.19	-0.46
Body mass index (kg/m^2)	-0.50	-0.57	-0.44
Lean body mass, James (kg)	-0.59	-0.63	-0.61
Ideal body weight (kg)	-0.44	-0.19	-0.46
Body surface area Mosteller (m^2)	-0.65	-0.67	-0.60

All correlation coefficients were statistically significant at the $p<0.0001$ level

Table 16. Aortic and hepatic enhancement (Hounsfield Units, HU) of iodixanol (320 mg I/ml) and iomeprol (400 mg I/ml), both injected at a dose of 40 grams of iodine and a dose rate of 1.6 gram iodine per second. Median values with 2.5 – 97.5 percentiles. The values shown have not been corrected for differences in sex and body parameters.

Parameters	Iodixanol (n=55)		Iomeprol (n=45)	
	Mean value	Median value (2.5 – 97.5 percentiles)	Mean value	Median value (2.5 – 97.5 percentiles)
Aorta, late arterial phase	233	232 (86-362)	229	199 (121-424)
Liver, parenchymal phase	65	65 (42-90)	63	59 (34-91)

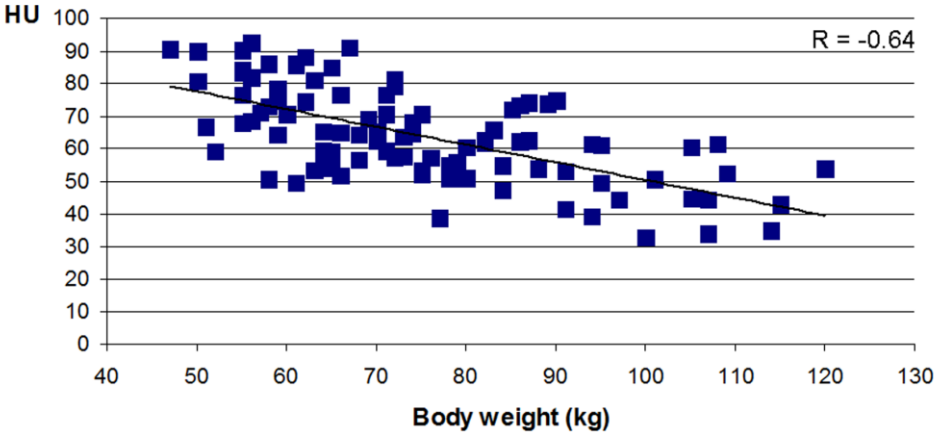

Figure 19. Liver parenchymal CM-enhancement as a function of BW.

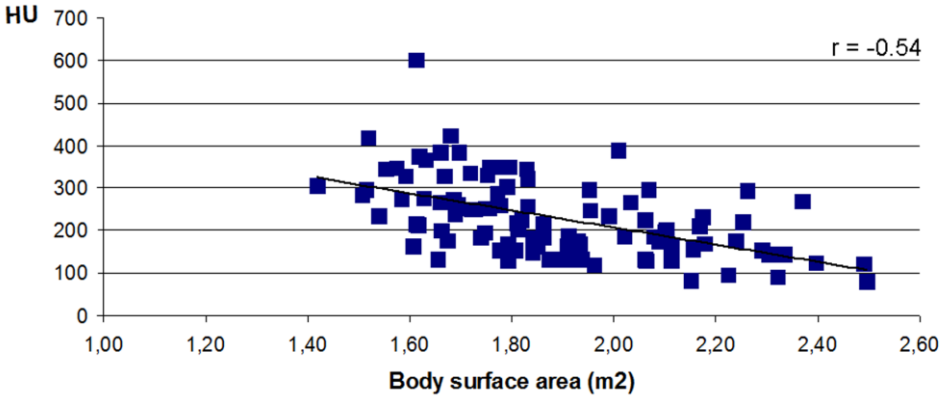

Figure 20. Aortic CM-enhancement as a function of BSA.

4.2.2 Comments

Differences in body size, expressed in BW, BSA or LBM, explained about 35-42% of the variability in liver enhancement and about 25-30% of the variability in aortic enhancement. Apparently, these measures of body size cannot explain all variation in CM-enhancement. A parameter that also might explain the variation in CM-enhancement could be CO, which was studied in Study IV. To compensate for differences in CO bolus tracking (smart prep) technique was used. However, the delay between the threshold value (HU-value) and the scanning of aorta was fixed to 20 seconds and for the liver another 25 seconds were added. Thus, the bolus tracking could not completely compensate for differences in CO.

As mentioned previously, a CM-enhancement of at least 50 HU is considered to be the minimum CM- enhancement for good diagnostic quality of the liver (133).
By using a fixed dose, this could not be achieved in 11 patients, indicating that an insufficient amount of CM was administered to these patients (BW males 84-115kg, median 97 kg , females 107 and 114 kg) (Figure 21). There were also patients in the other end of the spectrum, in whom the dosage of CM can be questioned due to a too high level of CM-enhancement. This was more explicit among females, where 18/42 had a liver CM-enhancement exceeding 70 HU in comparison to 16/58 in males.

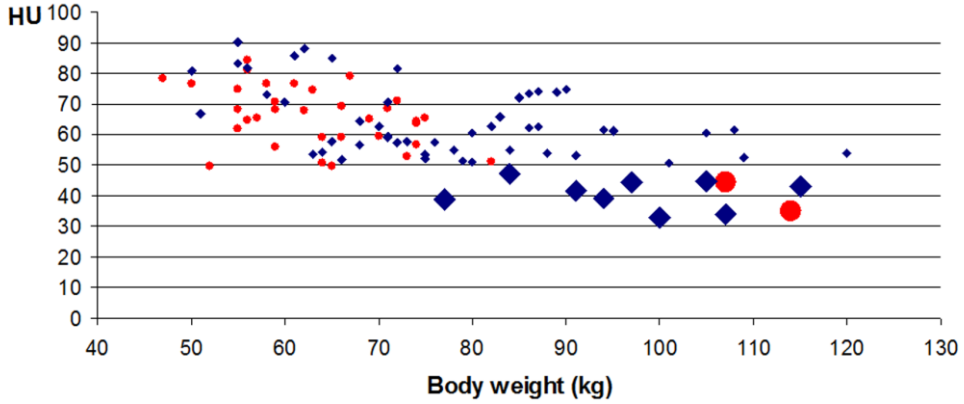

Figure 21. The relationship between CM enhancement of liver parenchyma and body weight. Note the 11 patients in whom insufficient CM-enhancement was achieved (9 males ♦ and 2 females ●).

4.3 Study III

4.3.1a Results, Group 1

Both studied parameters, BW and $CTDI_{vol}$, were inversely correlated to the hepatic CM-enhancement (Table 17) with no no statistically significant difference between the two parameters. As shown in Study II, gender did not have any influence on the relationship between CM-enhancement and BW, but such an influence was observed in the current study from $CTDI_{vol,}$ where r^2 increased from 0.35 to 0.37 after adjusting for gender ($p = 0.04$). There was no additive value of using both BW and $CTDI_{vol}$ in the regression model, nor of including age (Figure 22).

Table 17. Correlation between $CTDI_{vol}$, BW and liver parenchymal CM-enhancement.

Correlation	All (n=100)	Women (n=42)	Men (n=58)
Body weight (kg)	-0.64	-0.66	-0.57
$CTDI_{vol}$ (mGy)	-0.60	-0.62	-0.54

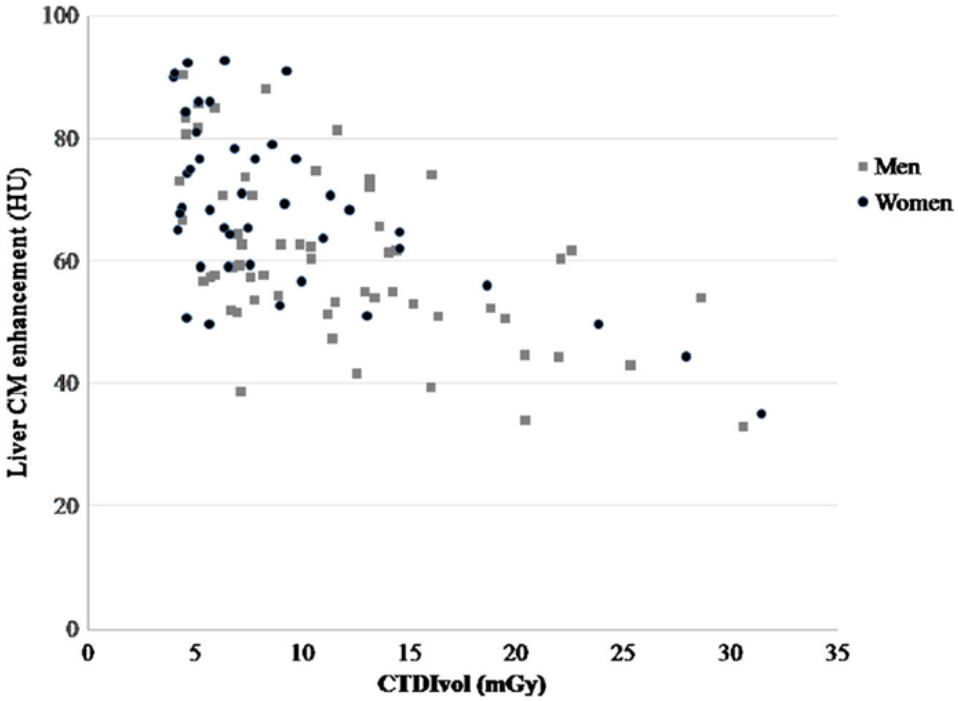

Figure 22. Liver parenchymal CM-enhancement as a function of $CTDI_{vol}$

4.3.1b Results, Group 2 (n=20)

A median CM-enhancement of liver of 68 (55-96) HU was achieved by individualising CM dose for $CTDI_{vol}$ using the formula based on the results from group 1. After adjusting CM for $CTDI_{vol}$ none of the patients had a CM-enhancement below 50 HU and no relationship between BW and hepatic CM-enhancement could be observed (Figure 23).

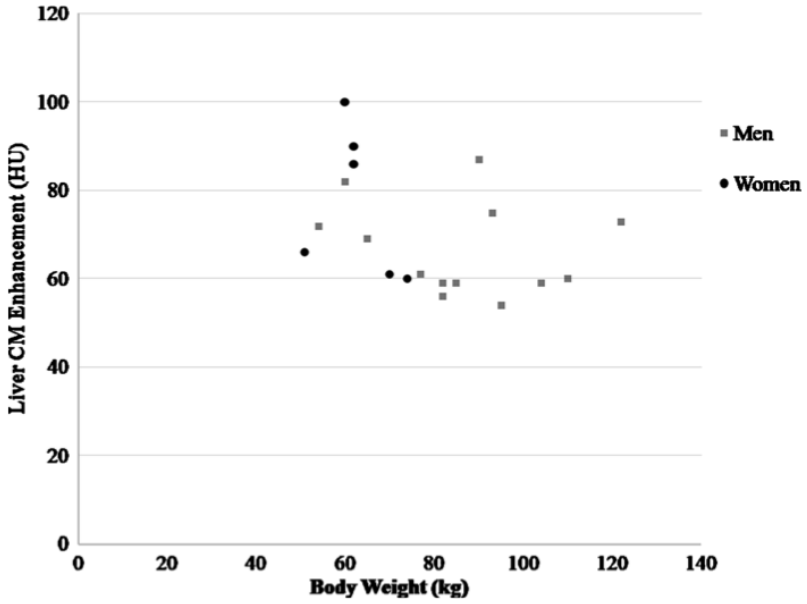

Figure 23. Relationship between BW and liver CM-enhancement during liver parenchymal phase in 20 patients. CM dosage was adjusted for $CTDI_{vol.}$

4.3.2 Comments

In this study the $CTDI_{vol}$ parameter was obtained from the actual exposure during the liver parenchymal phase, not from the scout images. In the clinical setting these data can evidently not be used individualizing CM dose. However, the difference between actual exposed $CTDI_{vol}$ and that estimated from the scout images is negligible.

Although performed successfully in group 2 in this study, using $CTDI_{vol}$ to individualize CM dosage must be performed with caution. Metal implants, keeping the arms alongside the body, or too high or too low positioning of the patients may result in incorrect $CTDI_{vol}$ values. Such methodological errors should be possible to reduce by automatic pattern recognition and subsequent adjustment. $CTDI_{vol}$ does also vary with the noise index used. This means that the $CTDI_{vol}$ will increase when a high radiation dose protocol is used and decrease for low dose protocols. A normalized NI should therefore be applied when adjusting the CM dose for body size using $CTDI_{vol}$. Thus, $CTDI_{vol}$ is simply used as a **"**body densitometry**"** of the examined patient.

4.4 Study IV

4.4.1 Results

The patient characteristics are presented in Table 18. The attenuation of ascending aorta, left atrium and inferior vena cava were similar between the groups, as were CO measurement (mean value 4.2 vs. 4.4 ml/min) and TTP (mean value 21 vs. 20.5 seconds).
A higher CM-enhancement of the left atrium in comparison to the ascending aorta was more frequent in group A than in group B (26 vs 14, $p < 0.05$) and their HR was significantly lower (mean value 58 vs. 62 BPM, $p < 0.05$).

There was an inverse relationship between BW and the attenuation of ascending aorta ($r = -0.55$, $p < 0.001$) (Figure 24). CO and stroke volume (SV), but not HR were related to the aortic attenuation (CO: $r = -0.30$ ($p<0.01$), SV: $r=-0.45$ ($p<0.001$) and HR: $r=0.10$ ($p=0.3$)).

After adjustment for the co-correlation of BW and CO on aortic attenuation the relationships remained (CO: $r=-0.27$ ($p<0.01$), SV: $r=-0.28$ ($p<0.01$) (Figure 25), HR: $r=-0.04$ ($p=0.7$)).

Table 18. Patient characteristics. Figures are given as mean value (standard deviation)

Parameters	Group A	Group B	Number (Group A/B)	Probability
Age (years)	58 (12)	57 (13)	50/50	NS
Female/Male	17/33	17/33	50/50	NS
Body weight (kg)	76 (12.0)	76 (12.4)	50/50	NS
Body height (cm)	177 (10.2)	175 (10.2)	50/50	NS
Cardiac output (CO, mL/min)	4.2 (0.8)	4.4 (1.1)	49/49	NS
Heart rate (BPM)	58 (9)	62 (9)	49/49	P<0.05
TTP (seconds)	21 (3.8)	20.5 (4.4)	46/46	NS
HU left atrium	433 (109)	416 (93)	50/50	NS
HU aorta	427 (88)	436 (90)	50/50	NS
HU inferior vena cava	81 (34)	79 (32)	50/50	NS
HU left atrium > HU Aorta (number)	26	14	50/50	P<0.05

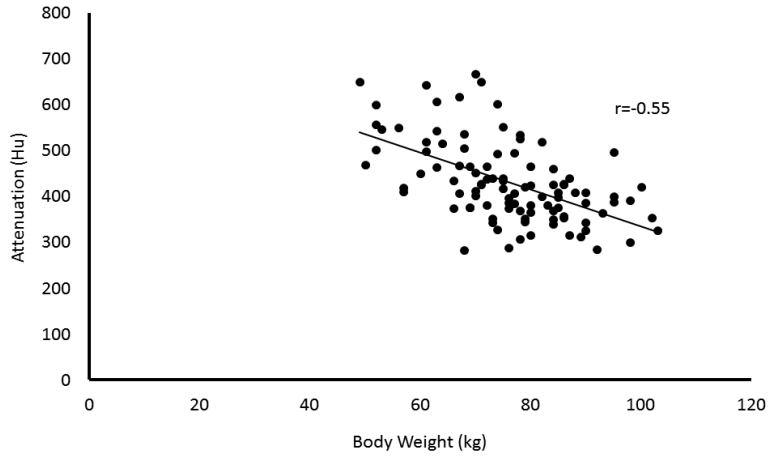

Figure 24. The relationship between contrast enhancement in aorta and BW.

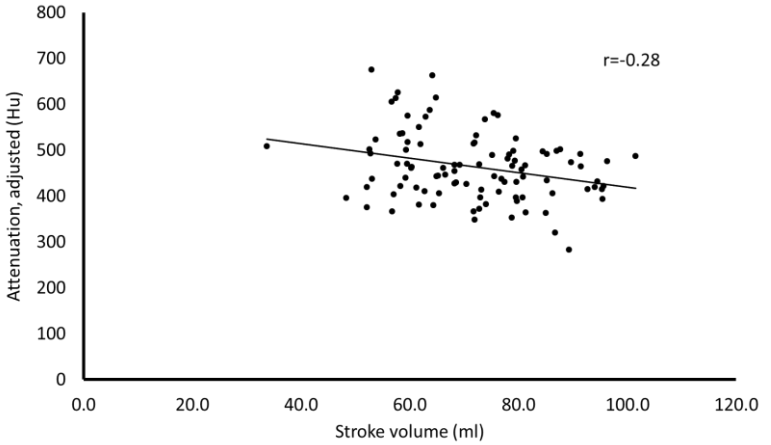

Figure 25. The relationship between aortic attenuation and stroke volume after normalization for BW.

4.4.2 Comments

There were no statistical differences in patient characteristics, CO nor HU enhancement of the inferior vena cava that could explain the higher frequency of too early imaging when the arms were placed above to the head than when resting on the CT front panel. Thus, in accordance with the hypothesis, the arm positioning affected the time for the CM to reach the heart. The observed higher HR when arms were placed ventrally could be due to the theoretically greater effort of holding the arms ventrally. Further studies are needed to elucidate this.
Interestingly, there was a correlation between CO (i.e. its component SV) obtained one minute prior to the CCTA examination and the CM-enhancement of the ascending aorta. This indicates that CO could be used for individualized dosing CM at CCTA.

5 Discussion

5.1 Heart rate variability and heat sensation at CT coronary angiography: Low-osmolar versus iso-osmolar contrast media (Study I)

The evaluation of the coronary vessels in Study I was challenging. When comparing the image quality between Study I and IV the difference is striking. This is due to differences in patient groups (where patients in Study I had strong suspicion of coronary disease while several subjects in Study IV were healthy volunteers), improvements in patient preparation (β-blocker and sublingual glyceryl nitrate to all patients), faster injection rates (5 and 6 ml/s) imaging strategy (retrospective gated analysis contra prospective ECG gating), and temporal resolution (175ms vs 75ms). The main technical issue was due to the use of retrospective gating when imaging the heart. The high number of HB necessary to cover the whole heart, ranging between 4-7 HB, resulted in a high frequency of HR changes during the acquisition, causing frequent image artefacts. Those can to a great extent be avoided by the improvements that have since been made. The CCTA examinations were also performed on two different generations of CT equipment with completely different performance, enabling several of the improvements listed above (GE Light Speed VCT vs. Siemens Somatom Definition Flash).

In study I there were no statistically significant differences between LOCM and IOCM groups in number of patients interfering with pre-defined scan protocol. However when analysing arrhythmic HB alone and when analysing HR exceeding 80 and 100 there were a significantly more arrhythmic HB when using the LOCM iomeprol than when using the IOCM iodixanol.
A study published a year after ours, with mainly the same objective and same type of CM, could not confirm our results (147). However, comparison was made on patient level, single arrhythmic HB were not studied and their patient population was considerably younger (> 18 years mean 58.5 years) than ours (> 50 years mean 63.5). However, another, more recently published study confirms our results, showing that LOCM gives more hemodynamic changes and stronger heat sensation than IOCM (148).

Patients in our LOCM group experienced a stronger heat sensation than those in the IOCM group (VAS 36 vs 18, p = <0.05). This complies with previous studies using LOCM and IOCM for CCTA (149). The discomfort of experiencing heat sensation may increase the HR, which in its turn will hamper the image quality on older 64 row MDCT systems. CCTA performed on more recent systems, which have a better temporal resolution and coverage, are probably less affected.

5.2 Hepatic CM-enhancement at CT and its correlation with various body size measures (Study II)

The fixed dose (¨one dose fit's all¨) strategy leads to a great variation in CM-enhancement of liver and aorta. By evaluating six different parameters describing body size it was shown that BW, LBM and BSA should be the suitable parameters for individualising CM dosage. In theory, if the CM dose had been adjusted for BW (mgI/kg BW) in our study approximately 40% of the variation in liver CM-enhancement could have been avoided.
Previous Japanese studies have reported a lower variation in hepatic parenchymal enhancement when using LBM in comparison to BW. However, their estimation of LBM was made using a body fat monitor (63-66), which may seem impractical in daily clinical practice.

The level of at least 50 HU has been advocated to be the target for sufficient diagnostic HU enhancement of the liver in parenchymal phase. To reach that level when individualising the CM dose based on BW a CM dose of approximately 521mgI/kg BW has been suggested (111). That dose corresponds well with the dose given to the patients in our study having HU values ranging between 50-70 HU. Their mean BW was 76 kg, resulting in an average iodine dose of 0.526mgI/kg.

As described previously, the VD increases with body size, but the vascularity varies among the tissues. The low VD of fat tissue can for example be observed at CT of the abdomen, where the fat tissue will have a negligible CM-enhancement after CM administration (57-59). This means that there is a potential risk that obese individuals will be given unnecessarily high doses when adjusting CM for BW. To reduce this risk a maximal CM dosage may be used e.g. 80 or 90 kg.

It has previously been shown that the best peak enhancement of the liver is achieved after a 25 seconds long CM injection (70). To obtain that injection duration in our study we therefore injected the 100 ml iomeprol 400 mgI/ml or 125 ml iodixanol 320 mgI/ml at a rate of 4 ml/s and 5 ml/s respectively. When adjusting the CM dose for body size the CM volume will vary. To keep the duration of the injection constant this implies that the injection rate will vary among the patients.

When differences associated with gender and body size parameters had been adjusted for it was apparent that iodixanol caused a significantly higher CM-enhancement in the liver in comparison with iomeprol ($p<0.01$). The most plausible explanation is that iomeprol is more diluted in the extracellular space secondary to its hypertonicity causing a shift of water from the intra- to the extracellular space, i.e. the plasma and the interstitial space of the liver. This presumed effect caused by the hypertonic iomeprol might be of importance when evaluating patients with edema. Similar differences in CM-enhancement have been observed previously at renal CT by Rasmussen et al, where a 10% lower dose of the dimer iodixanol resulted in no significant difference in CM-enhancement of aorta, vena cava and kidney compared to that of the monomer iopromide (125).

5.3 Automatic individualized contrast medium dosage at hepatic CT, by using computed tomography dose index volume ($CTDI_{vol}$) (Study III)

Improvement in CT technology has considerably shortened scan time. However, contrary to this, the administrative time devoted to each patient has increased e.g. documentation in radiological information system (RIS), patient journal system, calculation of individualized CM dosage etc. However, the collaboration between vendors of CT systems and CM injectors has led to the integration of injector software into the CT software. This includes the possibility to save dedicated injection protocols for each imaging protocol with automatic adjustment of the amount and injection rates of CM and saline, and it enables mixed saline and CM injections. As shown in this study, association between $CTDI_{vol}$ and the parenchymal CM-enhancement of the liver was not significantly inferior to that of BW. This implies that $CTDI_{vol}$ may be used instead of BW when adjusting CM dose for patient size. Such an approach has the potential to improve the efficiency of the patient logistics by enabling automated dosing of CM. Theoretically, the radiographer would in the future simply place the patient on the CT table and attach the patient to the auto injector. After confirmation of patient ID the system would then select the correct protocol, CM dosage and injection parameters automatically.

The hypothesis that CM dose may be automatically adjusted for body size by using $CTDI_{vol}$ was successfully tested in 20 patients. After CM dose adjustment there was no remaining relationship between BW and liver CM-enhancement (Fig. 18) and a liver CM-enhancement greater than 50 HU was obtained in all patients. However, this test was just made to prove the feasibility of the concept.

5.4 Timing and enhancement of intravenous contrast media at coronary computed tomography angiography: The effect of arm positioning, body weight and cardiac output (Study IV)

IV CM timing and HU enhancement are crucial factors in CCTA. In Study I and IV testbolus technique was used to define the optimum scan start after IV CM bolus injection. What distinguished these two studies was that in Study IV we used a 12-second pre-recorded respiratory instruction. The instruction began 17 seconds before scanning and ended 5 seconds before scanning. In Study I manual respiratory instruction was used which varied in the start and length.
When using the test bolus technique it is important that test bolus is performed under as similar conditions to the final scanning as possible, therefore by using a pre-recorded respiratory instruction influence from operator variability should be minimized.

The individual scan delay after CM injection at CCTA was defined by the TTP after test bolus injection, as described in 3.2.13.When analyzing the two different arm positions in Study IV, a higher frequency of patients with a higher attenuation in their left atrium than in the ascending aorta was observed when arms were held superiorly than when held ventrally. This relatively higher attenuation in the left atrium is observed when the imaging is made too early, i.e. when the scan delay is

too short. The probable reason for this underestimation of the necessary scan delay is that a relative occlusion of veins occur depending on the position of the arms. When performing the test bolus this obstruction is not significant enough to affect the time to peak, but when performing the CCTA scan twice the amount of fluid is given (60+50 ml compared to 15+40 ml). This greater amount probably results in a temporary stasis when arms are in superior position, but not in the ventral position.

In accordance with Study II and III the result of Study IV demonstrated a strong relationship between body size and IV CM-enhancement of the ascending aorta ranging from 283 HU to 667 HU. Clearly, the "one dose fits all" is not an optimal CM dosage strategy at CCTA. A clear relationship between body size and vessel enhancement at CCTA has previously been shown (124). Those findings are supported in our study where a correlation coefficient of -0.55 is observed when relating the attenuation to BW.
Interestingly the attenuation was also related to CO obtained one minute prior to imaging. This indicates that CO may be used as a means to individualize the IV CM dosage at CCTA. It may be hypothesized that individualizing CM dosage by adjusting for BW and CO in combination with an arm positioning ventral to the head may make it possible to reduce the amount of CM necessary for CCTA while maintaining an optimal contrast enhancement of the coronary arteries. Preliminary calculations show that the CM dose can potentially be halved in the smallest patients (data not shown), but larger and further studies are needed to define the optimal CM dosage strategy at CCTA.

6 CONCLUSIONS AND FINAL REMARKS

Study I:
Predefined HR during CCTA is not affected by the use of LOCM iomeprol or IOCM iodixanol. Using the same volume of CM but different amount of iodine did not affect the image quality assessment. When analysing the total number of irregular HB exceeding 80 and 100 HB, a significantly larger number of irregular HB in the LOCM group was observed ($p<0.001$). The use of LOCM was associated with a significantly higher level of experienced heat sensation. The results indicates that the use of IOCM iodixanol is more recommendable than the use LOCM iomeprol at retrospective gating in 64 row CCTA.

Study II:
The equations for BW, LBM and BSA showed the best correlation to HU-enhancement in liver and aorta in comparison to BH, BMI and IBW. To achieve a consistent hepatic enhancement, CM dose may simply be adjusted to body weight instead of using more complicated calculated parameters based on both weight and height. When adjusting for differences in weight, height, age and sex between the two groups there was a significantly stronger liver HU enhancement with iodixanol than that of iomeprol (mean difference 6 HU, $p < 0.01$).

Study III:
Liver parenchymal enhancement is related to $CTDI_{vol}$ and BW to a similar strength. Thus, BW may be replaced by $CTDI_{vol}$ as a method for adjusting CM doses to body size. The results indicate that in the future it would be potentially feasible to automatically individualize CM dosage by CT.

Study IV:
The standard positioning of the arms superior to the head at CCTA increases the risk of too early scanning after IV CM injection compared to when the arms are in a ventral position. However, the ten-second long CM injection used at CCTA gives a high success rate in terms of number of patients with sufficient enhancement of the coronary vessels. The great variability in CM enhancement and its good correlation to body size and cardiac output shows that the CM dose may be significantly reduced in most patients by taking those parameters into account.

7 ACKNOWLEDGEMENTS

Mi familia, Bernarda, **Alexander, Pierre y David,** son los mas importantes de mi vida.¡You os quiero mucho!
¨*If you look deeply into the palm of your hand, you will see your parents and all generations of your ancestors. All of them are alive in this moment. Each is present in your body. You are the continuation of each of these people*¨ *Thich Nhat Hanh*

This thesis would not have been possible without the guidance and help of several individuals who in one way or another contributed and extended their valuable assistance in the preparation and completion of these studies.

I would like to express my special appreciation and thanks to my principal supervisor **Torkel Brismar**, you have been a tremendous mentor for me. Thank you for your guidance, patience, optimism and encouragement.

I owe my deepest gratitude to my co-supervisor Professor **Peter Aspelin**. Thank you for giving me the opportunity and trust to fulfill this work.

Ulf Nyman, my co-supervisor, for his help of designing and manuscript writing in Study II-IV. Without his knowledge and assistance these studies would not have been successful.

Kerstin Cederlund, my co-supervisor, for her valuable suggestions during writing and finalizing of this thesis. I would also like to thank her for the cooperation regarding Study I, IV.

Kent Fridell, my mentor.

Jonas Björk, for his invaluable assistance in Study II-IV

My thanks and appreciation to my friend **Bertil Leidner.** It has been a privilege to work with you during all these years.

Jonaz Ripsweden, for his cooperation in Study I.

Nouhad Jallo, for her cooperation in Study II-IV, **Christian Werner**, for his cooperation in Study I.

Helena Forssell, for her valuable assistance during my years as a Ph.D. student.

Jessica Ekberg, for her assistance in connection with the dissertation.

Heads of Radiology department at Karolinska university hospital in Huddinge.

My thanks must go also to my friends **Ia Wassén** and **Lena Håkansson**.

8 REFERENCES

1) Oransky I. Sir Godfrey N Hounsfield. The Lancet 2004; 9439: 18-24

2) Seeram E. Computed tomography, physical principles, clinical applications and quality control. Second edition. Saunders Company 2001

3) Prokop M, Galanski M. Computed tomography of the body. Thieme Verlag 2003

4) Bates S, Beckmann L, Thomas A, Waltham R. Godfrey Hounsfield: Intuitive genius of CT. The British institute of radiology 2012

5) Neiman H, Lyons J. Fundamentals of angiography. Vascular Surgery Fifth Edition 2004;5:61-86

6) Skrepetis K, Siafakas I, Lykourinas M. Evolution of retrograde pyelography and excretory urography in the early 20th century. Journal of Endourology 2001;15:691-696

7) Osborne ED, Sutherland CG, Scholl AJ, Rowntree L. Roentgenography of urinary tract during excretion of sodium iodid. JAMA 1923;80:368-373

8) Almén T. The etiology of contrast medium reactions. Invest Radiol. 1994 May;29 Suppl 1:S37-45

9) Almén T. Contrast media: The relation of chemical structure, animal toxicity and adverse clinical effects. Am. J. Cardiol. 1990;66:2F-8F

10) Dawson P. Chemotoxicity of contrast media and clinical adverse effects. A review. Invest Radiol. 1985 ;20(1 Suppl):S84-91

11) Stoltberg HO, McLennan BL. Ionic versus noneionic contrast use. Curr Probl Diagn Radiol. 1991;20:47-88. Review.

12) Rappaport SI, Levitan H. Neurotoxicity of x-ray contrast media. Relation to lopid solubility and blood-brain barrier permeability. Am J Roentgenol Radium Ther Nucl Med.;122(1):186-93

13) Cicciarello R, d'Avella D, Mesiti F, Rosati G, Princi P, d'Aquino S, Hayes R. Effect of injections of contrast media on regional uptake of (14C)-2deoxyglucose by the rat brain. Brain Injury 1990;4:71-76

14) Caille J, Gioux M, Arné P, Paty J. Neurotoxicity of noneionic iodinated water-souble contrast media in myelography: Experimental study. AJR 1982;4:1185-1189

15) Koeda T, Motegi I, Ichikawa T, Suzuki T, Kato M. Changes in hemodynamic due to the contrast medium during left ventriculography. Angiology 1987;38:825-32

16) Green CE, Higgins CB, Kelley MJ, Newell JD, Schmidt WS, Haigler F. Effects of intracoronary administration of contrast materials on left ventricular function in presence of severe coronary artery stenosis. Cardiovasc Intervent Radiol. 1981;4:110-116

17) Singh J, Daftary A. Iodinated Contrast Media and Their Adverse Reactions. J Nucl Med Technol. 2008;36:69-74

18) Brinker J. What every cardiologist should know about intravascular contrast. Rev Cardiovasc Med. 2003;4(suppl 5):S19-S27

19) Almén T. Visipaque a step forward. A historical review. Acta Radiologica Suppl. 1995;399:2-18

20) Caulfield JB, Zir L, Harthorne JW. Blood calcium levels in the presence of arteriographic contrast material. Circulation 1975;52:119-123

21) Brunette J, Mongrain R, Rodhés-Cabau J, Larose É, Leask R, Bertrand OF. Comperative Rheology of low- and iso-osmolarity contrast agents at different temperatures. Catheterization and cardiovascular interventions 2008;71:78-83

22) Hund J. Determination of viscosity. Metal Finishing 2002;100:630-632

23) Dyvik K. Dyrstad K, Tronstad A. Relationship between viscosity and determined injection pressure in angiography catheters for common roentgen contrast media. Acta Radiologica 1995;Suppl. 399:43-49

24) Cademartiri F, Mollet NR, van der Lugt A, McFadden EP, Stijnen T, de Feyter PJ, Krestin GP. Intravenous contrast material administration at helical 16-detector row CT coronary angiography: effect of iodine concentration on vascular attenuation. Radiology. 2005;236:661-665

25) Harnoy A. Bearing design in machinery. Taylor & Francis 2005

26) Stacul F, Molen A, Reimer P, Webb J, Thomsen H, Morcos S, Almén T, Aspelin P, Bellin M, Clement O, Heinz-Peer G. Contrast induced nephropathy: Updated ESUR contrast media safety Committee guidelines. Eur Radiol 2011;21:2527-2541

27) Kormano M, Partanen K, Soimakallio S, Kivimaeki T. Dynamic contrast enhancement of the upper abdomen: Effect of contrast medium and body weight. Invest. Radiol. 1983;18:364-367

28) Kormano M, Dean, P. Extravascular contrast material: The major component of contrast enhancement. Radiology 1976;121:379-382

29) Yasuyuki Y, Yasuyuki K, Mutsumasa T, Masufami U, Naofumi H, Tadafumi S, Isamu N. Abdominal helical CT: Evaluation of optimal doses of intravenous contrast material-A prospective randomized study. Radiology 2000; 216:718-723

30) Dean PB, Violante MR, Mahoney JA. Hepatic CT contrast enhancement: Effect of dose, duration of infusion, and time elapsed following infusion. Invest. Radiol. 1980; 15:158-161

31) Berland LL, Lee JY. Comparison of contrast media injection rates and volumes for hepatic dynamic incremental computed tomography. Invest. Radiol. 1988; 23:918-922

32) Claussen CD, Banzer D, Pfretzschner C, Kalender WA, Schörner W. Bolus geometry and dynamics after intravenous contrast medium injection. Radiology;153:365-368

33) Heiken JP, Brink JA, McClennan BL, Sagel SS, Crowe TM, Gaines MV. Dynamic incremental CT: Effect of volume and concentration of contrast material and patient weight on hepatic enhancement. Radiology 1995;195:353-357

34) Bae KT. Intravenous Contrast Medium Administration and Scan Timing at CT: Considerations and Approaches. Radiology 2010;256:32-61

35) Ehman E, Guimaraes L, Fidler J, Takahashi N, Giraldo J, Yu L, Manduca A, Huprich J, McCollough, Holmes D, Harmsen S, Fletcher J. Noise reduction to decrease radiation dose and improve conspicuity of hepatic lesions at contrast-enhanced 80-kV hepatic CT using projection space denoising. AJR Am J Roentgenol 2012;198:405-411

36) Krestin G, Glazer G. Advances in CT IV. Springer-Verlag 1998

37) Bonomo L, Foley D, Imhof H, Rubin G. Multidetector computed tomography technology: Advances in imaging techniques. The Royal Society of Medicin Press Limited 2003

38) Goldman L. Principles of CT: Multislice CT. Journal of Nuclear Medicine Technology 2008; 36: 57-68

39) Bonomo L, Foley D, Imhof H, Rubin G. Multidetector computed tomography technology: Advances in imaging techniques. The Royal Society of Medicin Press Limited 2003

40) Saini S, Rubin G, Kalra M. MDCT a practical approach. Springer-Verlag 2006

41) Hoe J, Toh KH. First experience with 320-row multidetector CT coronary angiography scanning with prospective electrocardiogram gating to reduce radiation dose. J Cardiovasc Comput Tomogr. 2009;3:257-61

42) Hsiao EM, Rybicki FJ, Steigner M. CT coronary angiography: 256-slice and 320-detector row scanners. Curr Cardiol Rep 2010;12:68–75

43) Karçaaltıncaba M, Aktaş A. Dual energy CT revisited with multidetector CT: A review of principles and clinical applications. Diagn Interv Radiol 2011; 17:181–194

44) Gabbai M, Leichter I, Mahgerefteh S, Sosna J. Spectral material characterization with dual-energy CT: Comparison of Commercial and investigative technologies in phantoms. Acta Radiol 2014;Online:1-10

45) Morgan K. Rolf M. Sievert: The pioneer in the field of radiation protection. Health Physics 1976;31:263

46) Huda W. A radiation exposure index for CT. Radiation protection dosimetry 2013; 157: 172-180

47) Zhonghua S. Radiation dose measurements in coronary CT angiography. World J Cardiol 2013;5:459-464

48) Shope T, Gagne R, Johnson G. A method for describing the doses delivered by transmission x-ray computed tomography. Med Phys 1981;8:488-495

49) Lee C, Goo J, Lee H, Ye S, Park C, Chun E, Im J. Radiation dose modulation techniques in multidetector CT era: From basis to practice. RadioGraphics 2008;28:1451-1459

50) Söderberg M, Gunnarsson M. Automatic exposure control in computed tomography- An evaluation of systems from different manufacturers. Acta Radiologica 2010;51:625-634

51) Kaasalainen T, Palmu K, Reijonen V, Kortesniemi. Effect of patient centering on patient dose and image noise in chest CT. AJR 2014; 203: 123-130

52) Keiser R, Reyisson P, Mulligan T. Definition of signal-to-noise ratio and its critical role in split-beam measurements. Mar. Sci 2005; 62 (1): 123-130

53) Nyman U, Leitz W, Kristiansson M, Påhlstorp P-Å. Stråldosreglering vid kroppsdatortomografi. SSI-rapport 2004:12

54) Flohr TG, Ohnesorge BM. Imaging of the heart with computed tomography. Basic Res. Cardiol. 2008;103:161-173

55) Hurlock G, Higashino H, Mochizuki T. History of cardiac computed tomography: Singel to 320-detector row multislice computed tomography. Int J Cardiovasc Imaging 2009;25:31–42

56) Kachelreis M. Phase-correlated dynamic CT. Biomedical Imaging 2004;1:616-619

57) Takao M, Masanori T, Thoshiaki H, Atsushi Y, Eiji N, Tohru Y. Radiation dose reduction and coronary assessabiliy of prospective electrocardiogram-gated computed tomography coronary angiography: Comparison with

retrospective electrocardiogram-gated helical scan. Journal of the American College of Cardiology 2008;52:1450-1455

58) Feyter P, Krestin G. Computed tomography of the coronary arteries. Taylor & Francis 2005

59) Halliburton SS. Recent technology advances in multi-detector row cardiac CT. Cardiol Clin. 2009;27:655-64

60) Kroft LJ, Roos A, Geleijns J. Artifacts in ECG-synchronized MDCT coronary angiography. AJR 2007;189:581–591

61) Earls JP. How to use a prospective gated technique for cardiac CT. J Cardiovasc Comput Tomogr. 2009;3:45-51

62) Sun G, Li M, Li L, Li G, Zhang H, Peng Z. Optimal systolic and diastolic reconstruction windows for coronary CT angiography using 320-detector rows dynamic volume CT. Clinical Radiology 2011;66:614-620

63) Goo H. State of the art CT imaging techniques for congenital heart disease. Korean J Radiol 2010;11:4-18

64) Ohnesorg B, Becker C, Flohr T, Reiser M. Multislice CT in cardiac imaging. Springer-Verlag 2002

65) Flohr T, Leng S, Yu L, Allmendinger T, Bruder H, Petersilka M, Eusemann C, Steirstorfer K, Schmidt B, McCollough C. Dual source spiral CT with pitch up to 3.2 and 75 ms temporal resolution: Image reconstruction and assessment of image quality. Med. Phys. 2009;36:5641-5653

66) Sun Z. Coronary CT angiography with prospective ECG-triggering: An effective alternative to invasive coronary angiography. Cardiovasc Diagn Ther 2012;2:28-37

67) Xu L, Yang L, Zhang Z. Low-dose adaptive sequential scan for dual-source CT coronary angiography in patients with high heart rates: Comparison with retrospective ECG gating. Eur J Radiol 2010;76:183-187

68) Nakaura T, Awai K, Yanaga Y. Low-dose contrast protocol using the test bolus technique for 64-detector computed tomography coronary angiography. Jpn J Radiol 2011; 29:457–465

69) Weininger M, Barraza M, Kemper C. Cardiothoracic CT angiography: Current contrast medium delivery strategies. AJR 2011; 196:W260–W272

70) Seifarth H, Puesken M, Kalafut J. Introduction of an individually optimized protocol for the injection of contrast medium for coronary CT angiography. Eur Radiol 2009; 19: 2373–2382

71) Sun K, Liu G, Li Y. Intravenous contrast material administration at high-pitch dual-source CT coronary angiography: Bolus-tracking technique with shortened time of respiratory instruction versus test bolus technique. Chin Med Sci 2012; 27:225-231

72) Wuest W, Zunker C, Anders K, Ropers D, Achenbach S, Bautz W, Kuettner A. Functional cardiac imaging: A new contrast application strategy for a better visualization of the cardiac chambers. European Journal of Radiology 2008;68:392–397

73) Kerl JM, Ravenel JG, Nguyen SA, Suranyi P, Thilo C, Costello P, Bautz W, Schoepf UJ. Right heart: Split-bolus injection of diluted contrast medium for visualization of coronary CT angiography. Radiology 2008**;**247:356–364

74) Jin-guo L, Xiong-biao C, Xiang T, Shi-liang, Ru-ping D. What is the best contrast injection protocol for 64-row multi-detector cardiac computed tomography? European Journal of Radiology 2010;75:159–165

75) Nicol ED, Arcuri N, Rubens MB, Padley SP. Considerations when introducing a new cardiac MDCT service. Avoiding the pitfalls. Clinical Radiology 2008; 63:355-369

76) Bettman MA, Bourdillon PD, Barry WH, Brush KA, Levin DC. Contrast agents for cardiac angiography: Effect of a nonionic agent vs. a standard ionic agent. Radiology 1984;153:583-587

77) Morettin LB, Zhan X, Ambrogio FB, Ambrogio G. Cardiorespiratory responses elicited by right atrial injections of iodinated contrast media. Invest. Radiol. 1994;29:201-209

78) Kinnison ML, Powe NR, Steinberg EP. Results of randomized controlled trials of low-versus high-osmolality contrast media. Radiology 1989;170:381-389

79) Mancini GB, Bloomqvist JN, Bhargava V, Stein JB, Lew W, Slutsky RA, Shabetai R, Higgins CB. Hemodynamic and electrocardiographic effects in man of a new noneionic agent (iohexol): Advatages over standard ionic agents. The American Journal of Cardiology 1983;51:1218-1222

80) Bergstra A, Dijk RB, Brekke O, Buurma AE, Orozco L, Heijer P, Crijns HJ. Hemodynamic effects of iodixanol and iohexol during ventriculography in patients with compromised left ventricular function. Catheterization and cardiovascular interventions 2000;50:314-321

81) Flinck A, Selin K, Björneld L, Nossen JO. Iodixanol and iohexol in cardioangiography. A comperative vectorcardiographic study. Acta Radiologica 2000;41:384-389

82) Dahlström K, Shaw DD, Clauss W, Andrew E, Sveen K. Summary of U.S. and European intravascular experience with iohexol based on clinical trial program. Invest. Radiol. 1985;20 (1 Suppl):S117-21

83) Manke C, Marcus C, Page A, Puey J, Batakis O, Fog A. Pain in femoral arteriography. A double-blind, randomized, clinical study comparing safety and efficacy of iso-osmolar iodixanol 270 mgI/ml and the low osmolar iomperol 300 mgI/ml in 9 European centers. Acta Radiologica 2003;44:590-596

84) McCullough, PA,Capasso P. Patient discomfort associated with the use of intra-arterial iodinated contrast media: A metea-analysis of comparative randomized controlled trials. BMC Med Imaging 2011;24:12

85) Stacul F. Current iodinated contrast media. Eur Radiol. 2001;11:690-697

86) Torrance GW, Feeny D, Furlong W. Visual analog scales: Do they have a role in the measurement of preferences for healt states. Med Decis Making 2001;21:329-334

87) DeLoach LJ, Higgins MS, Caplan AB, Stiff J. The visual analog scale in the immediate postoperative period: Intrasubject variability and correlation with a numeric scale. Anesth Analg 1998;86:102-106

88) Borg G. Många symptomskalor håller inte måttet. Läkartidningen 2013; 110: CF94

89) Fishman EK. Multidetector-row computed tomography to detect coronary artery disease: The importance of heart rate. European Heart Journal Suppl. 2005;7:G4-G12

90) Nicol ED, Arcuri N, Rubens MB, Padley SP. Considerations when introducing a new cardiac MDCT service. Avoiding the pitfalls. Clinical Radiology 2008; 63:355-369

91) Abbara S, Arbab-Zadeh A, Callister T, Desai M, Mamuya W, Thomson L, Weigold G. SCCT guidelines for performance of coronary computed tomographic angiography: A report of the society of cardiovascular computed tomography guidelines committee. Journal of cardiovascular computed tomography. 2009; 3: 190-204

92) Zhang J, Fletcher JG, Scott W, Araoz PA, Williamson EE, Primak AN, McCollough CH. Analysis of heart rate and heart rate variation during cardiac CT examination. Acad Radiol. 2008;15:40-48

93) Chen X, Chen T, Yun F, Huang Y, Li J. Effect of repetitive end-inpiration breath holding on very short-term heart rate variability in heathy humans. Physiol. Meas. 2014;35:2429-2445

94) Pai MP, Paloucek FP. The origin of the ¨ideal¨ body weight equations. Ann Pharmacother 2000;34:1066-1069

95) Shah B, Sucher K, Hollenbeck CB. Comparison of ideal body weight equations and published height-weight tables with body mass index tables for health adults in the United States. Nutrition in Clinical Practice 2006;21:312-319

96) Eknoyan G. Adolphe Quetelet (1796-1874)-the average man and indices of obesity. Nephrol Dial Transplant 2008;23:47-51

97) No authors listed. Clinical Guidelines on the Identification, Evaluation, and Treatment of Overweight and Obesity in Adults--The Evidence Report. National Institutes of Health. Obes Res. 1998;6:461-2.

98) Devine B. Gentamacin therapy. Drug Intelligence and Clinical Pharmacy 1974;8:650-655

99) Leykin Y, Pellis T, Lucca M, Lomangio G, Marzano B, Gullo A. The pharmodynamic effects of rocuronium when dosed according to real body weight or ideal body weight in morbidly obese patients. Anesth Analg 2004;99:1086 –1090)

100) Langebrake C, Bernhard F, Baehr M, Kröger N, Zander AR. Drug dosing and monitoring in obese patients undergoing allogenic stem cell transplantation. Int J Pharm 2011;33:918-924

101) Forbes GB, Hursh JB. Age and sex trends in lean body mass calculated from K^{40} measurements: With note on the theoretical basis for the procedure. Ann N Y Acad Sci. 1963;26;110:255-63

102) Segal K, Loan M, Fitzgerald P, Hogdon J, Van T. Lean body mass estimation by bioelectrical impedance analysis: A four-site cross-validation study. Am J Clin Nutr 1988;47:7-14

103) Hume R. Prediction of lean body mass from height and weight. J. Clin. Path. 1966;19:389-391

104) James, W. P. T. Research on Obesity.1976 Her Majesty's Stationery Office, London

105) Ritchie CB, Davidson RT. Regional body composition in college-aged Caucasians from anthropometric measures. Nutrition & Metabolism 2007; 4:29

106) Du Bois E. Clinical calorimetry. A formula to estimate the approximate surface area if height and weight be known. Archives of Internal Medicin 1916;17:303-3011

107) Cosolo WC, Morgan DJ, Seeman E, Zimet AS, McKendrick JJ, Zalcberg JR. Lean body mass, body surface area and epirubicin kinetics. Anticancer drugs 1994;5:293-297

108) Daniels S. Indexing left ventricular mass to account for differences in body size in children and adolecents without cardiovascular disease. Am J Cardiol 1995;76:699-701

109) Hallnyck E, Soepp H, Thomis J, Boelaept J, Daneels R, Dettili L. Should clearance be normalized to body surface area or to lean body mass. Br J Clin Pharmacol 1981;11:523-526

110) Mosteller RD, Simplified calculation of body surface area. N Engl J Med 1987;317:1098

111) Verbraecken J, Heyning P, De Backer W, Van Gaal L. Body surface area in normal-weight, overweight, and obese adults. A comparison study. Metabolism Clinical and Experimental 2006;55:515-524

112) Kondo H, Kanematsu M, Goshima S, Tomita Y, Miyoshi T, Hatcho A, Moriyama N, Onozuka M, Shiratori Y, Bae K. Abdominal multidetector CT in patients with varying body fat percentages: Estimation of optimal contrast material dose. Radiology 2008;249:872-877

113) Bonaldi VM, Bret PM, Reinhold C, Atri M. Helical CT of the liver: Value of an early hepatic arterial phase. Radiology 1995;197:357-363

114) Mitsuzaki K, Yamashita Y, Ogata I, Nishiharu T, Urata J, Takahashi M. Multiple-phase helical CT of the liver detecting small hepatomas in patient with liver chrrosis: Contrast-injection protocol and optimal timing. AJR 1996;167:753-757

115) Awai K, Inoue M, Yagyu Y, Watanabe M, Sano T, Nin S, Koike R, Nishimura Y, Yamashita Y. Moderate versus high concentration of contrast material for aortic and hepatic enhancement and tumor-to-liver contrast at multi-detector row CT. Radiology 2004;233:682-688

116) Allen T, Peng TH, Chen K, Huang T, Chang C, Fang H. Prediction of blood volume and adiposity in man from body weight and cume of height. Metabolism 1956;5:328-344

117) Ertl AC, Diedrich A, Raj SR. Techniques used for the determination of blood volume. Am Med Sci 2007;334:32-36

118) Yanaga Y, Awai K, Nakayama Y, Nakaura T, Tamura Y, Hatemura M, Yamashita Y. Pancreas: Patient body weight-tailored contrast material injection protocol versus fixed dose protocol at dynamic CT. Radiology 2007;245:475-482

119) Awai K, Hori S. Effect of contrast injection protocol with dose tailored to patient weight and fixed injection duration on aortic and hepatic enhancement at multidetector-row helical CT. Eur. Radiol. 2003;13:2155-2160

120) Nyman U, Almén T, Jacobsson B, Aspelin P. Are intravenous injections of contrast media really less nephrotoxic than intra-arterial injections? Eur Radiol. 2012: DOI 10.1007/s00330-011-2371-4

121) Yamashita Y, Komohara Y, Takahashi M, Uchida M, Hayabuchi N, Shimizu T, Narabayashi I. Abdominal helical CT: Evaluation of optimal doses of intravenous contrast material-A prospective randomized study. Radiology 2000;216:718-723

122) Kondo H, Kanematsu M, Goshima S, Tomita Y, Kim M, Moriyama N, Onozuka M, Shiratori Y, Bae K. Body size indexes for optimizing iodine dose for aortic and hepatic enhancement at multidetector CT: Comparison of total body weight, lean body weight and blood volume. Radiology 2009;254:163-169

123) Yanaga Y, Awai K, Nakaura T, Utsunomiya D, Oda S, Hirai T, Yamashita Y. Contrast material injection protocol with dose adjusted to the body surface area for MDCT aortography. AJR 2010;194:903-908

124) Bae KT, Seeck BA, Hildebolt CF, Tao C, Zhu F, Kanematsu M, Woodard PK. Contrast enhancement in cardiovascular MDCT: Effect of body weight, height, body surface area, body mass index, and obesity. AJR 2008;190:777-784

125) Ho LM, Nelson RC, Delong DM. Determining contrast medium dose and rate on basis of lean body weight: Does this strategy improve patient-to-patient uniformity of hepatic enhancement during multi-detector row CT. Radiology 2007;243:431-437

126) Awai K, Hiraishi K, Shinichi H. Effect of contrast material injection duration and rate on aortic peak time and peak enhancement at dynamic CT involving injection protocol with dose tailored to patient weight. Radiology 2004;230:142-150

127) Yanaga Y, Awai K, Nakaura T, Oda S, Funama Y, Bae KT, Yamashita Y. Effect of contrast injection protocols with dose adjusted to estimated lean body weight on aortic enhancement at CT angiography. AJR 2009;192:1071-1078

128) Yanaga Y, Awai K, Nakayama Y, Nakaura T, Tamura Y, Hatemura M, Yamashita Y. Pancreas: Patient body weight-tailored contrast material injection protocol versus fixed dose protocol at dynamic CT. Radiology 2007;245:475-482

129) Ichikawa T, Erturk S, Araki T. Multiphasic contrast-enhanced multidetector-row CT of liver: Contrast-enhancement theory and practical scan protocol with a combination of fixed injection duration and patients body-weight-tailored dose of contrast material. European Journal of Radiology 2006;58:165-176

130) Awai K, Hori S. Effect of contrast injection protocol with dose tailored to patient weight and fixed injection duration on aortic and hepatic enhancement at multidetector-row CT. Eur Radiol 2003;13:2155-2160

131) Guo D, Bian J. Multislice spiral CT angiography in evaluation of liver transplantation candidates. Hepatobiliary Pancreat Dis Int. 2005;4:32-36

132) Chambers TP, Baron RL, Lush RM. Hepatic CT enhancement: Part I. Alteration in the contrast material volume and rate of injection within the same patients. Radiology 1994; 193: 513-517

133) Heiken JP, Brink JA, McClennan BL, Sagel SS, Crowe TM, Gaines MV. Dynamic incremental CT: Effect of volume and concentration of contrast material and patient weight on hepatic enhancement. Radiology 1995; 195: 353-357

134) Chambers TP, Baron RL, Lush RM. Hepatic CT enhancement: Part II. Alterations in contrast material volume and rate of injection within the same patients. Radiology 1994; 193:518-522

135) Bae KT, Heiken J, Brink JP. Aortic and hepatic contrast medium enhancement at CT. Part II. Effect of reduced cardiac output in a porcine model. Radiology 1998;207:657-662

136) Kondo H, Kanematsu M, Goshima S, Miyoshi T, Shiratori Y, Onozuka M, Moriyama N, Bae K. MDCT of the pancreas: Optimizing scanning delay with a bolus tracking technique for pancreatic, peripancreatic vascular, and hepatic contrast enhancement. AJR 2007;188:751–756

137) Tan C, Low A, Thng C. APASL and AASLD consensus guidelines on imaging diagnosis of hepatocellular carcinoma: A review. Int J Hepatol. 2011;2011:519783

138) Kim M, Choi J, Lim J, Kim J, Kim J, Oh Y, Yoo E, Chung J, Kim K. Optimal scan window for detection of hypervascular hepatocellular carcinomas durin MDCT examnination. AJR 2006;187:198–206

139) Goshima S, Kanematsu M, Kondo H, Yokoyama R, Miyoshi T, Nishibori H, Kato H, Hoshi H, Onozuka M, Moriyama N. MDCT of the liver and hypervascular hepatocellular carcinomas: Optimizing scan delays for bolus-tracking techniques of hepatic ariterial and portal venous phases. AJR 2006; 187:W25–W32

140) Kanematsu M, Goshima S, Kondo H, Nishibori H, Kato H, Yokoyama R, Miyoshi T, Hoshi H, Onozuka M, Moriyama N. Optimizing scan delays of fixed duration contrast injection in contrast-enhanced biphasic multidetector-row CT for the liver and the detection of hypervascular hepatocellular carcinoma. J Comput Assist Tomogr 2005;29:195–201

141) Russo A, VanPutte C, Regan J. Seelýs essentials of anatomy & physiology. Seven edition, McGraw Hill Companies (2009) ISBN 978-0077361389

142) Cockcroft DW, Gault MH. Prediction of creatinine clearance from serum creatinine. Nephron 1976;16:31-41

143) Nyman U, Björk J, Sterner G, Bäck SE, Carlson J, Linström V, Bakoush O, Grubb A. Standardization of p-creatinine assays and use of lean body mass allow improved prediction of calculated glomerular filtration rate in adults: A new equation. Scand J Clin Lab Invest 2006;66:451-468

144) Halliburton SS, Abbara S. Practical tips and tricks in cardiovascular computed tomography: patient preparation for optimization of cardiovascular CT data acquisition. J Cardiovasc Comput Tomogr. 2007;1:62-625

145) Budoff M, Shinbane J. Handbook of cardiovascular CT: Essentials for clinical practice. Springer –Verlag 2008;2:15

146) Austen WG, Edwards JE, Frye RL, Gensini GG, Gott VL, Griffith LS, McGoon DC, Murphy ML. A reporting system on patients evaluated fot coronary artery disease. Report of the Ad Hoc Committee for Grading of Coronary Artery Disease, Council on Cardiovascular Surgery, American Heart Association. Circulation 1975;51:5-40

147) Becker C, Vanzulli A, Fink C, Faveri D, Fedeli S, Dore R, Biondetti P, Kuettner A, Krix M, Ascenti G. Multicenter comparison of high concentration contrast agent iomperol-400 with iso-osmolar iodixanol-320. Contrast enhancement and heart rate variation in coronary dual-source computed tomographic angiography. Investigative Radiology 2011;46:457-464

148) Andreini D, Pontone G, Mushtaq S, Barttorelli A, Conte E, Bertella E, Baggiano A, Annoni A, Formenti A, Ballerini G, Agostini P, Fiorentini C, Pepi M. Coronary stent evaluation with coronary computed tomographic angiography: Comparison between low-osmolar, high-iodine concentration iomeprol-400 and iso-osmolar, lower-iodine concentration iodixanol-320. J of cardiovasc. comput. Tomography 2014;8:44-51

149) Ozbulbul N, Yurdakul M, Tola M. Comparison of a low-osmolar contrast medium iopamidol, and iso-osmolar contrast medium, iodixanol, in MDCT coronary angiography. Coron Artery Dis. 2010;21:414-9